Progress in Hyperspectral Remote Sensing Science and Technology in China Over the Past Three Decades

Qingxi Tong, Yongqi Xue, and Lifu Zhang, *Member, IEEE*

***Abstract*—This paper reviews progress in hyperspectral remote sensing (HRS) in China, focusing on the past three decades. China has made great achievements since starting in this promising field in the early 1980s. A series of advanced hyperspectral imaging systems ranging from ground to airborne and satellite platforms have been designed, built, and operated. These include the field imaging spectrometer system (FISS), the Modular Airborne Imaging Spectrometer (MAIS), and the Chang'E-I Interferometer Spectrometer (IIM). In addition to developing sensors, Chinese scientists have proposed various novel image processing techniques. Applications of hyperspectral imaging in China have been also performed including mineral exploration in the Qilian Mountains and oil exploration in Xinjiang province. To promote the development of HRS, many generic and professional software tools have been developed. These tools such as the Hyperspectral Image Processing and Analysis System (HIPAS) incorporate a number of special algorithms and features designed to take advantage of the wealth of information contained in HRS data, allowing them to meet the demands of both common users and researchers in the scientific community.**

***Index Terms*—Hyperspectral remote sensing, imaging spectrometry, remote sensing technology, remote sensing applications.**

I. Introduction

HYPERSPECTRAL imaging, also known as imaging spectrometry or imaging spectroscopy, has become established as a critical technique for Earth observation since it was first proposed by A.F.H. Goetz in the 1980s [1]. Imaging spectroscopy began a revolution in remote sensing by combining traditional two-dimensional imaging remote sensing technology and spectroscopy [1]–[3], allowing for the synchronous acquisition of both images and spectra of objects. Hyperspectral images contain a wealth of geo- and radiometric information as well as abundance spectral information for narrow spectral bands (typically about $10^{-2}\,\lambda$) from the ultraviolet and visible to shortwave infrared for each pixel. Hyperspectral remote sensing (HRS) has greatly improved our ability to qualitatively and quantitatively sense the Earth and outer space and has therefore attracted growing interest from researchers worldwide. HRS has been used successfully in various applications including agriculture, forestry monitoring, food security, natural resources surveying, vegetation observation, and geological mapping.

Hyperspectral data are obtained from ground, airborne, or spaceborne measurements, such as by the Airborne Visible/Infrared Imaging Spectrometer (AVIRIS) and the EO-1 Hyperion (both launched by NASA). They generally consist of tens to hundreds of contiguous spectral bands with narrow bandwidths of typically about $10^{-2}\,\lambda$. The special characteristics of hyperspectral datasets make HRS of the Earth and outer space an appealing but challenging prospect. Much pioneering work in the HRS community has focused on developing new algorithms, models, and tools for data processing. These techniques greatly facilitate the understanding and quantitative analysis of HRS and have been employed in various applications, such as target detection [4], precise classification [5], and quantitative retrieval [6].

China, as one of the pioneers in HRS technology development, has made great achievements since the 1980s. To meet the increasing demand for fast and precise surveying and mapping of natural resources on a large scale, many outstanding hyperspectral sensors have been designed and launched in China (particularly on aircraft) with the support of various national major projects. Some of them, such as the Modular Airborne Imaging Spectrometer (MAIS), the Pushbroom Hyperspectral Imager (PHI), and the Operational Modular Imaging Spectrometer (OMIS-I and OMIS-II), played important roles in cooperative projects between China and the USA, France, Australia, Japan, and Malaysia during the 1990s. As a result, these sensors are well known worldwide and opened opportunities for high-tech international cooperation in this field in China. The development and improvement of the MAIS, in particular, has been reported internationally, including in the "Chevron Hyperspectral Brochure and White Paper" (http://www-old.cstars.ucdavis.edu/projects/chevronwhitepaper/). To make use of these excellent hyperspectral instruments, a number of advanced techniques and software for hyperspectral imaging processing have also been developed in China and have aided national goals such as resource exploration.

Manuscript received August 29, 2012; revised November 20, 2012 and May 05, 2013; accepted June 02, 2013. Date of publication July 22, 2013; date of current version December 18, 2013. This work was supported by the National Natural Science Foundation of China (Grant 41072248 and Grant 41101328) and the National High Technology Research and Development Program of China (863 Program) under Grant 2012AA12A301. *(Corresponding author: L. Zhang.)*

Q. Tong and L. Zhang are with the Institute of Remote Sensing and Digital Earth, Chinese Academy of Sciences, Beijing 100101, China (e-mail: tqxi@263.net; zhanglf@irsa.ac.cn).

Y. Xue is with the Shanghai Institute of Technical Physics, Chinese Academy of Sciences, Shanghai 2000083, China (e-mail: xueyongqi_cas@126.com).

Color versions of one or more of the figures in this paper are available online at http://ieeexplore.ieee.org.

Digital Object Identifier 10.1109/JSTARS.2013.2267204

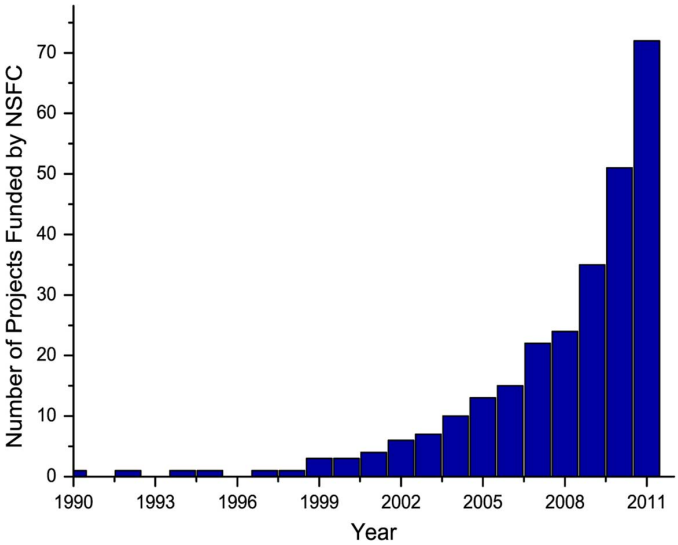

Fig. 1. Number of projects supported by the NSFC from 1990 to 2011 (data taken from http://www.nsfc.gov.cn/Portal0/default152.htm).

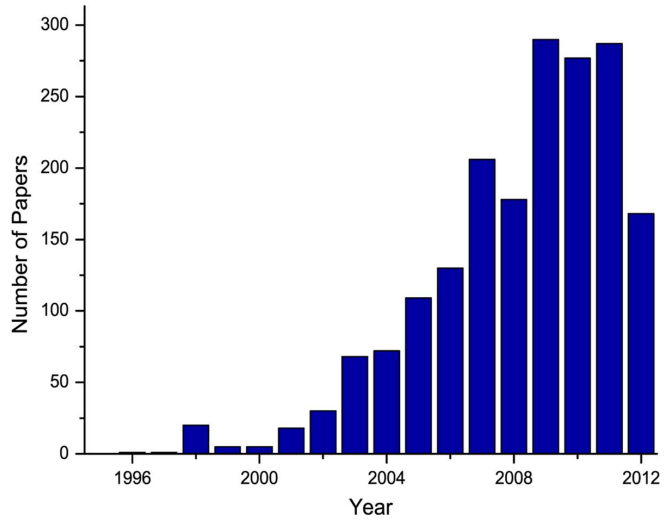

Fig. 2. High-quality papers related to HRS written by Chinese scientists from 1995 to September 2012 (data taken from Web of Science).

High-performance hyperspectral sensors with high signal to noise ratio (SNR), fine spectral resolution, and wide spectral ranges and swathes have been designed in China since the early 2000s. During this period, spaceborne imaging spectrometers such as the Chinese Moderate-Resolution Imaging Spectroradiometer (CMODIS) have been developed, launched, and operated. These kinds of sensors provide new insights into various aspects of the Earth on a large scale, but they also bring new challenges for analysis because of the massive amounts and complexity of the obtained hyperspectral data [7]. To overcome the 'dimensionality curse' of hyperspectral data, various image processing techniques have been investigated for specific applications in China. All these novel sensors and techniques have been used in many applications that are related to geoscience.

Over the last 30 years, the rapid development of HRS and related technologies has been greatly aided by increased attention from the Chinese government, as evidenced by the increasing number of projects closely related to HRS supported by the National Natural Science Foundation of China (NSFC) from 1990 to 2011 (see Fig. 1). As a result, an increasing number of researchers have started work on HRS and its applications. Fig. 2 shows the statistics of high-quality papers related to HRS published by Chinese researchers and scientists from 1995 to September 2012. The original data are from the Web of Science (http://wokinfo.com/). The yearly growing trend of papers published is obvious from Fig. 2.

This paper describes the progress in HRS in China, with a particular focus on the past three decades. Much outstanding work in this field has been conducted by Chinese scientists, and it is difficult to cover all of it. As a result, only work selected from high-quality journals, conferences, books, monographs, and websites is reviewed here. This paper is organized as follows. Section II presents advances in imaging spectrometers on ground, airborne, and spaceborne platforms. Section III introduces hyperspectral imagery processing techniques, and Section IV presents selected typical applications of hyperspectral imaging. Finally, software and generic tools developed for hyperspectral data are described in Section V. The conclusion and prospects for future work are given in Section VI.

II. Advances in Imaging Spectrometers

Widespread use of hyperspectral imaging technologies ultimately depends on the development of more technically advanced hyperspectral sensors to ensure the availability of high-quality imaging data. Since the beginning of the 1980s, with advances in hyperspectral imaging mechanisms and related technologies such as optical imaging and diffraction technology, China has successfully installed many imaging spectrometers on ground, airborne, and spaceborne platforms. Most of these sensors are listed in Table I. The most representative ones are described here in detail. The ground-based, airborne, and spaceborne sensors described in this paper are in most cases imaging spectrometers. These differ from "point-record" remote sensing instruments such as the distinguished Analytical Spectral Devices (ASD) FieldSpec Pro FR.

A. Ground-Based Imaging Spectrometers

To meet the increasing demands for field measurements, many research groups and universities in China have begun to design operational ground-based imaging spectrometers over the past decade. Some pioneering research groups have reported on the prototypes of field-portable hyperspectral imagers. These include institutions of the Chinese Academy of Sciences (CAS), such as the Institute of Remote Sensing Applications (IRSA), the Shanghai Institute of Technical Physics (SITP), and the Anhui Institute of Optics and Fine Mechanics (AIOFM). In addition, the University of Science and Technology of China, Beihang University, Beijing Institute of Technology, and Nanjing Center of China Geological Survey have made significant contributions to the development of such devices.

Among these ground-based instruments is a novel Field Imaging Spectrometer System (FISS) developed by IRSA, CAS, in 2008. The FISS is considered to be the first sensor for field imaging spectrometry developed in China. Table II lists the main technical parameters of the FISS. The FISS [8], [9], which was built with a two-dimensional cooled-array charge-coupled device (CCD) camera, was specially designed for ground or

TABLE I
OVERVIEW OF HYPERSPECTRAL IMAGERS IN CHINA

Sensor	Spectral Coverage /μm	Spectral Res. /nm	No. of Bands	Available Date
Airborne hyperspectral imaging sensor				
AMSS	8.0–12.0	210	19	1986–1990
FIMS	2.035–2.380	30	12	1985
MAIS	0.44–1.08 1.5–2.45 8.0–11.6	20 25 450	32 32 7	1987-1990
PHI-I	0.4–0.85	< 5	244	1990s
OMIS-I	0.46–1.1 1.06–1.70 2.0–2.5 3.0–5.0 8.0–12.5	10 40 15 250 500	64 16 32 8 8	1995
OMIS-II	0.4–1.1 1.55–1.75 2.08–2.35 3.0–5.0 8.0–12.5	10 200 270 2000 4000	64 1 1 1 1	2001
WHI	0.41–0.98	< 5	124	2003
Spaceborne hyperspectral imaging sensor				
CMODIS	0.4-12.5	20	34	2002
HJ-1A HSI	0.45–0.95	5	115	2008
FY-3 MERSI	0.44–0.89 0.39–1.04 1.62-2.15 10-12.5	50 20 50 2500	5 12 2 1	2008
Chang'E-1 IIM	0.48-0.96	15	32	2009
TG-1 HSI	0.40-1.0	10	-	2011
Sensor	Spectral Coverage /μm	Spectral Res. /nm	No. of Bands	Available Date
	1.0-2.5	23		
Ground-based hyperspectral imaging sensor				
FISS	0.4-0.9	5	344	2008

elevated car-mounted remote sensing. Although the FISS is based on concepts of the Pushbroom Hyperspectral Imager (PHI) [10], the new system is distinguished from the PHI and other hyperspectral push-broom sensors in its acquisition of a second spatial dimension. Instead of moving forward, the sensor uses a scan mirror within a certain angle and record rate driven by a stepper motor assembled in the FISS. Fig. 3 shows a schematic of the FISS, indicating the key imaging processes from reflected radiance (incoming photons) to digital images. Using a 464×344 CCD chip, the FISS measures incoming radiation in 344 contiguous spectral channels in the 437–902 nm wavelength range with a spectral resolution of better than 5 nm. It creates images of 464 pixels for a line of targets with a nominal instantaneous field of view (IFOV) of ~1 mrad.

The FISS can be used both in the laboratory under artificial light and under natural field conditions. It can be mounted onto a ground-based multi-use platform or an elevated car, as shown in Fig. 4. The IRSA, CAS, was granted an invention patent for the FISS in 2010 ("A Field Imaging Spectrometer System," patent No. ZL201010130916.0).

Since its creation, the FISS has been rigorously tested and spectrally, geometrically, and radiometrically calibrated in the laboratory. Primary research [8], [9] on the FISS indicates that it is a potentially powerful tool for ground-based remote sensing. This was further confirmed by initial applications [8], [11], [12], including crop-weed discrimination, milk identification, and biochemical and biophysical parameter estimation

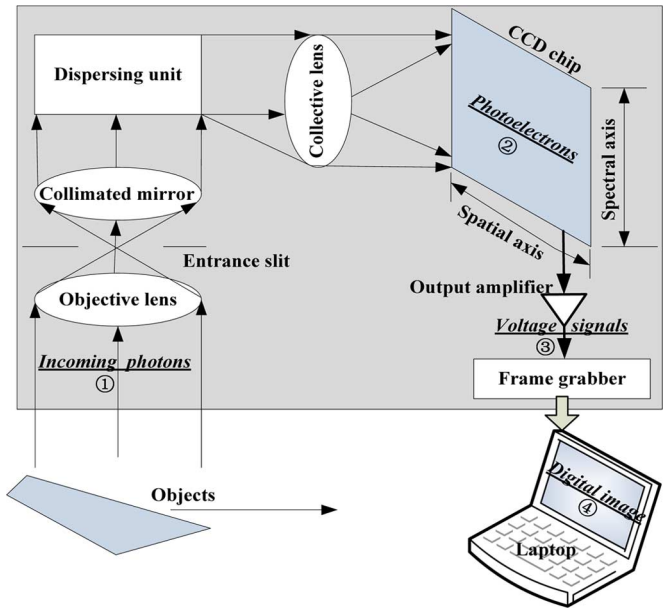

Fig. 3. Schematic of the FISS.

TABLE II
MAIN TECHNICAL PARAMETERS OF THE FISS

Number of bands	344	Imaging rate	Maximum 20 frames/s
Spectral range	437–902 nm	Scan field	–20° to +20°
Spectral resolution	Better than 5 nm	Quantitative value	12 bit
Spatial resolution	About 1 mrad	Signal to noise ratio	>500:1 (60% bands)
Radiometric calibration	Better than 5%	Spectral sampling interval	About 1.4 nm

of vegetation by researchers of the IRSA, CAS. More recently, Huang *et al.* proposed a system-setting-based radiometric calibration (RC) model for the FISS [13]. This may improve its radiometric calibration efficiency greatly, and thus promote its wider use in quantitative applications.

B. Airborne Hyperspectral Devices

Since 1991, when the modular airborne imaging spectrometer (MAIS) was successfully tested in Darwin, Australia, China has initiated the development of aero-imaging spectrometry. It has become an important member of the international aviation hyperspectral remote sensing society, launching many distinguished airborne hyperspectral sensors with increased bands, spectral resolution, and SNRs, such as the PHI and OMIS series. Recently, because of the demand for emergency precise monitoring of natural disasters and high-quality remotely sensed images that incorporate geometrical, radiometrical, and spectral information, new hyperspectral imaging systems have been assembled and designed in China.

1) Modular Airborne Imaging Spectrometer (MAIS): The MAIS instrument was designed, built, and operated by SITP of the CAS. The instrument is the first real imaging spectrometer in China. It features 71 spectral channels with a spectral coverage from 0.44 μm to 11.8 μm. The MAIS consists of a tilted

Fig. 4. The FISS at work: (left) situated on a ground-based multi-use platform and (right) mounted on an elevated car.

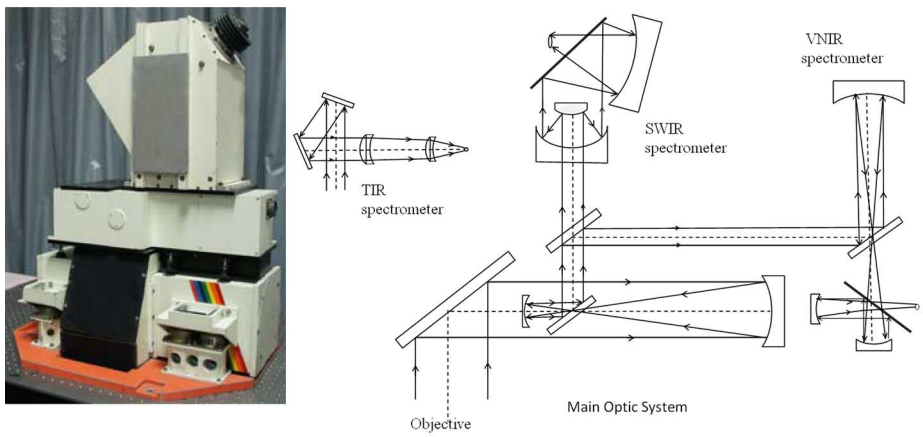

Fig. 5. The MAIS sensor and its optical system.

TABLE III
BASIC TECHNICAL SPECIFICATIONS OF THE MAIS

	VIS-NIR	SWIR	TIR
Spectral range	0.44–1.08 μm	1.5–2.5 μm	8.2–12.2 μm
Spectral channel	32	32	7
Spectral resolution	20 nm	25 nm	450 nm
IFOV	3 mrad	4.5 mrad	3 mrad

45-degree rotation mirror optical scanning unit and three spectrometer modules for different spectral ranges. The main optical system of the MAIS is shown in Fig. 5, and its basic technical specifications are listed in Table III.

During the period September–October 1991, the MAIS was installed on a Citation S/II aircraft of the CAS and flown successfully in a joint Sino-Australian remote sensing campaign near Darwin and at several other test sites in western Australia. In addition, the MAIS has also been widely used for geological and environmental surveys in China.

2) Operational Modular Imaging Spectrometer (OMIS): The OMIS developed by SITP of the CAS has two modes, OMIS-I and OMIS-II. It is based on the MAIS and hence retains some of its features, such as modular restrictions. The two operating modes feature different technical performances, as shown in Table IV. Fig. 6 shows the OMIS-I sensor. Apart from spectrometers, a high-quality difference GPS was assembled in the OMIS system to yield a positioning accuracy of better than 10 m.

3) Pushbroom Hyperspectral Imager (PHI): Pushbroom hyperspectral imaging is an excellent method to acquire imaging spectral data using focal plane technology. As shown in Fig. 7, the fore-optics collects lights reflected from the ground. The length and width of the entrance slit affect the spectral resolution and swath. The incoming electromagnetic radiation will be separated into distinct angles. The spectrum of a single ground pixel is dispersed and focused at different locations in one dimension of the detector array. The number of pixels is equal to the number of ground cells for a given swath. The motion of the aircraft provides the scan along-track direction. The inverse of the line frequency is therefore equal to the pixel dwell time.

The PHI collects spectral images using a grating. There are two kinds of diffraction grating used in the design of the PHI: reflective and transmission. Specifications of the three kinds of PHI are listed in Table V.

4) Unmanned Aerial Vehicle (UAV)-Based Hyperspectral Imaging System: A UAV-based hyperspectral imaging system was integrated with an unmanned helicopter GC-201 and a self-developed aerial imaging spectrometer. This system can cover the full spectral range, providing data from multispectral sensors, digital cameras, and GPS. Fig. 8 shows a sketch of the new UAV-based hyperspectral imaging system, which was developed in China with the support of a special project for environmental monitoring and protection. Compared to traditional hyperspectral payloads on manned aircraft or satellites, the main advantages of the UAV-based hyperspectral

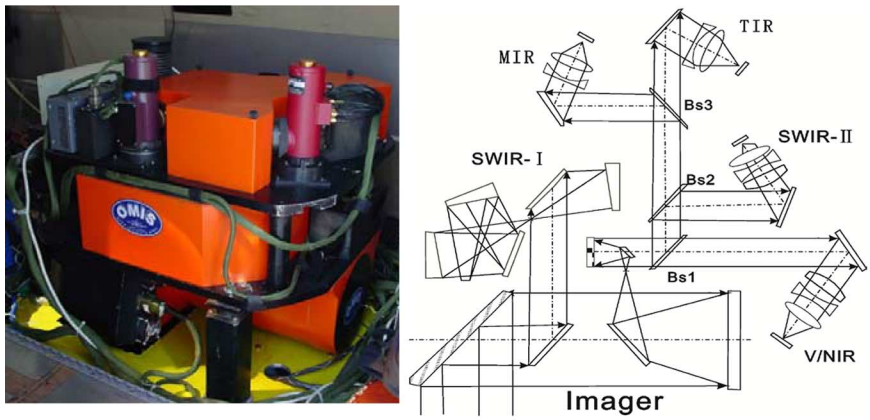

Fig. 6. The OMIS-I sensor and schematic.

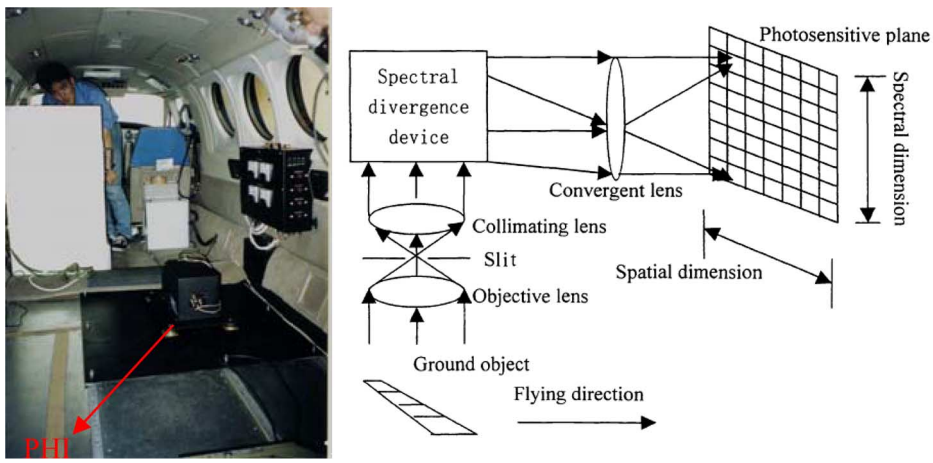

Fig. 7. The PHI sensor on the "King Air" aircraft and its imaging principle.

TABLE IV
SPECIFICATIONS OF THE OMIS

OMIS-I			OMIS-II		
Spectral range / μm	Spectral resolution / nm	Band	Spectral range / μm	Spectral resolution / nm	Band
0.46–1.1	10	64	0.44–1.1	10	64
1.06–1.70	40	16	1.55–1.75	200	1
2.0–2.5	15	32	2.08–2.35	270	1
3.0–5.0	250	8	3.0–5.0	2000	1
8.0–12.5	500	8	8.0–12.5	4000	1
IFOV (mrad)	3		IFOV (mrad)	1.5/3 (optional)	
FOV/Digit			78 degree/12 bit		

imaging system are its increased flexibility, cost-effectiveness, and low weight, which make it useful for performing frequent monitoring of agriculture, forestry, and water resources. In particular, the UAV-based remote sensing system may have unique advantages in natural disaster monitoring, detection, and assessment by providing high spatial, spectral, and temporal resolution images. UAV-based remote sensing systems are rapidly moving into the mainstream of the research field and are therefore an appealing research topic.

To accelerate the development of hyperspectral imaging techniques, advanced airborne imaging spectrometers such as the CASI, SASI, and TASI, which cover the full spectral range, have also been introduced from the Canadian company ITRES. These sensors have been modified and assembled into a comprehensive hyperspectral imaging acquisition and processing system by the CNNC, Beijing Research Institute of Uranium Geology.

C. Spaceborne Hyperspectral Imagers

In 2000, the Hyperion imaging spectrometer aboard the EO-1 mission of the NASA New Millennium Program started the era of hyperspectral remote sensing of the Earth from space. The Hyperion sensor provides 220 contiguous spectral bands that cover a wide spectral range (400–2500 nm) with a narrow spectral resolution (10 nm). Hyperion, the first real spaceborne imaging spectrometer, has achieved acceptable performance and initiated hyperspectral remote sensing applications at a global scale [14]. Keeping up with the international pace, China has also developed and launched a series of spaceborne hyperspectral imagers during the past three decades. These sensors were specifically designed for various purposes with different technical parameters.

1) SZ-3 CMODIS: CMODIS is a Chinese Moderate Resolution Imaging Spectroradiometer aboard the Shenzhou-3 (SZ-3) Spaceship of the China National Space Agency (CNSA) launched in March 2002. CMODIS, like MODIS launched by NASA in 1999, provides a total of 34 spectral bands covering the 0.4–12.5 μm spectral region [15]. The main specifications of CMODIS are given in Table VI.

TABLE V
SPECIFICATIONS OF THE PHI

	PHI-1	PHI-2	PHI-3
Spectral Range	400–800 nm	400–870 nm	410–980 nm
Spectral Band	244	247	124
Spectral Sample Interval	1.8 nm	1.9 nm	
Spectral Resolution	< 5 nm	< 5 nm	< 5 nm
FOV	21°	23°	42°
Spatial Samples	376	652	1304
IFOV	1.5°	1.2° (0.6°)	0.6°
Dynamic Range	12 bits	14 bits	14 bits
Maximum Scan Rate	60 fps	50 fps	50 fps
Cooling	No	Yes	Yes
Grating Class	Reflective	Transmission	Transmission

Fig. 8. The UAV-based hyperspectral imaging system.

TABLE VI
MAIN SPECIFICATIONS OF THE CMODIS

	VIS/NIR	SWIR		TIR
Spectral range (μm)	0.403–0.803/0.843–1.043	2.15–2.25	8.4–8.9	10.3–11.3/11.5–12.5
	(20 bands/10 bands)	1 band	1band	1 band/1band
Spectral resolution (μm)	20 nm	0.1	0.5	0.5
SNR	≥250	≥200	≤0.4k	≤0.8k
Spatial resolution	400–500 m (334 ± 5 km orbit height)			
FOV/Digitization	440/12 bit			

CMODIS was designed mainly for remote sensing of ocean or water color from Earth orbit. However, other applications in vegetation observation, geological surveying, land use/cover mapping, and change detection have also been reported. The results indicate that the CMODIS can provide an effective and reliable data source for remote sensing applications. Fig. 9 shows a hyperspectral image of the Yangtze River obtained by CMODIS. In the image, Dongting and Poyang lakes can be clearly seen attached to the Yangtze River.

2) Chang'E-1 IIM: Chang'E-1, an unmanned spacecraft designed for lunar exploration, was launched on 24 Oct. 2007 as China's first lunar mission under the support of China's Lunar Exploration Program (CLEP). To achieve its science goals, Chang'E-1 carried eight sets of scientific instruments. The Sagnac-based Interferometer Spectrometer (IIM), which used an interference pattern to acquire a spectrum, was developed to retrieve the chemical and mineral composition of the lunar surface. The IIM is a hyperspectral imager that covered nearly 84% of the moon surface from 70°N to 70°S using 32 spectral bands within the wavelength range of 480–960 nm. The basic imaging principle of the IIM was introduced by Wu *et al.* [16], as shown in Fig. 10. Its main technical characteristics are described in Table VII.

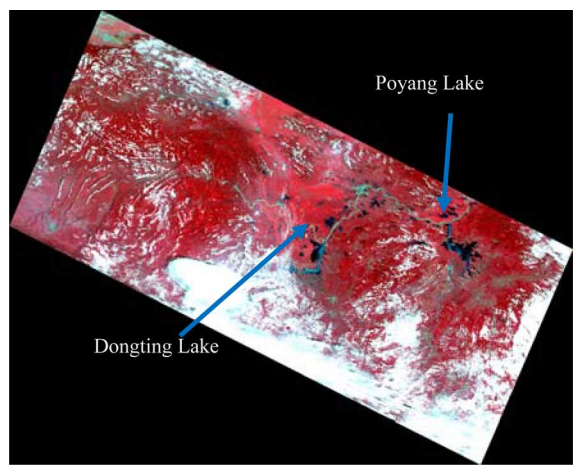

Fig. 9. CMODIS hyperspectral image of the Yangtze River: standard false color in the order of Red: band 21(853 nm), Green: band 15 (693 nm) and Blue: band 8 (553 nm).

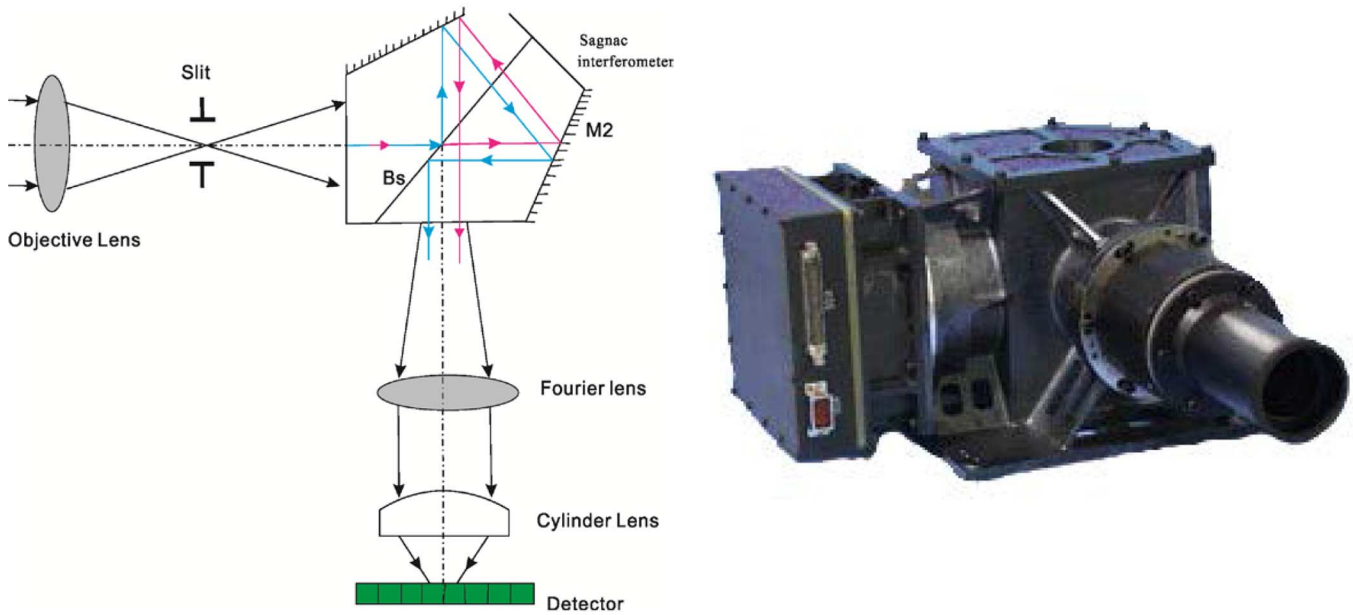

Fig. 10. Schematic of The IIM (left) and the IIM sensor (right) [16].

TABLE VII
MAIN TECHNICAL CHARACTERISTICS OF THE IIM

Spectral channel	32	Spectral resolution	325.5cm^{-1}
Spatial resolution	200 m	Spectral range	480–960 nm
Swath width	25.6 km	Imaging region	70°N–70°S
SNR	≥100	Orbit altitude	200 km
Digitization	12 bit	Pixel number	256*256

The Chang'E-1 IIM ended its mission on 1 March 2009. During its 495-day life-span, a large number of lunar hyper-spectral data were collected. Using the IIM data, Wu *et al.* presented global high-spatial-resolution maps of lunar iron and titanium contents, which agreed closely with the results derived from the Clementine ultraviolet-visible (UVVIS) data [16].

3) FY-3 MERSI: Following the meteorological FengYun-1 (FY-1) series and FY-2 series, FY-3A, the second generation of Chinese polar-orbit meteorological satellites, was launched on 27 May 2008. One difference between the previous FY series and the FY-3A is that the latter carried 11 scientific instruments, which allowed it to obtain multi/hyper-spectral, three-dimensional, quantitative environmental parameters on the land, ocean, and atmosphere in all weather conditions from a near-polar, sun-synchronous orbit at a nominal altitude of 836 km. Among the sensors aboard FY-3A, the Medium-Resolution Spectral Imager (MERSI), which features 20 spectral channels from the visible/infrared (0.4–2.1 μm divided by 19 channels) to thermal infrared (10–12.5 μm), is considered a milestone satellite sensor from China. Its distinguished capabilities include gapless global observation and high radiometric performance with two internal calibrator systems. Table VIII lists the basic technical indices of FY-3A/MERSI. Because of MERSI's global observation abilities, it can be used to investigate global climate change and achieve objectives such as color remote sensing for algae bloom monitoring and coastal suspended sediment mapping.

TABLE VIII
BASIC TECHNICAL INDICES OF FY-3A/MERSI

Spectral region	0.4–12.5 μm	Spectral region	20
Scanning range	± 55.40	Spatial resolution	0.25–1 km
Quantization	12 bit	Radiometric calibration accuracy	<7%, 0.4–2.1 μm <1K, 10–12.5 μm
Assembling two onboard calibrator systems: one for 0.4-2.1 μm, the other for 10–12.5 μm			

Fig. 11. The HJ-1A HSI sensor.

4) HJ-1A HSI: The HJ-1A is a member of the Chinese HJ-1 small satellite constellation (HJ-1A/1B). It was successfully launched on 6 Sept. 2008 for environment and disaster monitoring and forecasting. The HJ-1A is equipped with a CCD camera and a Hyper-Spectral Imager (HSI). The HSI acquires surface features in 115 contiguous spectral bands in the 450–950 nm wavelength range with a spectral resolution of about 5 nm. The HSI can achieve a wider swath than the EO-1 Hyperion (50 km), but it has a smaller ground instantaneous field of view (100 m). Fig. 11 shows the HJ-1A HSI sensor.

5) Other Hyperspectral Imagers: An advanced hyperspectral imager jointly developed by two institutions from CAS, including the Changchun Institute of Optics, Fine Mechanics and Physics (CIOMP) and SITP, was launched on 29 Sept. 2011 onboard China's first target vehicle Tiangong-1 (TG-1). Up to now, the instrument has operated more than 6000 hours in its orbit and obtained a number of hyperspectral images that have been successfully applied in environmental monitoring of the Earth (http://www.cmse.gov.cn/news/show.php?itemid=2555). These applications demonstrate that the TG-1 HSI has achieved high performance levels in spatial, spectral, and SNR.

Now, China is also cooperating with Germany on the CarbonSat Constellation Programme, which aims to develop a small constellation of satellites to measure methane and carbon dioxide levels in the atmosphere.

III. Hyperspectral Image Processing Techniques

As discussed in Section I, hyperspectral images have unique advantages over traditional multispectral or panchromatic remotely sensed images. They can detect, identify, and discriminate surface features of interest through the contiguous spectrum (spectral signature) of each pixel. These advantages have inspired the development of new techniques for hyperspectral data processing. Techniques such as spectral unmixing or spectral matching may be less effective for single/multi-spectral images resulting from only a few separate spectral bands. However, hyperspectral images also have disadvantages. These include the Hughes [17]–[19] and high redundancy [20], [21] phenomena, and the widespread mixture effect [22], [23]. To overcome these problems, new analytical processing techniques must be developed. This section reviews the recent advances in hyperspectral image processing and analysis techniques in China, including spectral matching, feature selection and extraction, spectral unmixing, data fusion [24]–[28], and super-resolution reconstruction [29].

A. Spectral Matching

The spectral matching technique is well known in the HRS community. It uses the contiguous spectral curves extracted from hyperspectral data to discriminate, identify, or detect targets of interest. These techniques, which include the spectral angle mapper (SAM), binary coding (BC), and spectral derivative feature coding (SDFC), have been widely applied to hyperspectral signature discrimination and data classification. To improve classification accuracy, researchers have tried to modify traditional spectral matching techniques over the past decades. He *et al.* [30] proposed an improved similarity measure called the weight SAM that sets a weight in the large difference spectral range between similar minerals, to further increase their discriminability. Fang *et al.* [31] combined the spectral distance and spectral shape to construct a spectral similarity scale. Their work was based on the dynamic weight adjustment method (SDW) and avoided the shortcomings of the single similarity measure. More recently, interdisciplinary theories, especially from biology, have also been introduced to improve spectral matching techniques. For example, Jiao *et al.* [32] proposed an artificial biological deoxyribonucleic acid (DNA) computing-based spectral encoding and matching algorithm to implement hyperspectral image classification. The DNA encoding classifier takes the advantages of spectral signatures and optimizes the matching process while avoiding interference from spectral diversity. Hence it far outperforms traditional classification methods [33].

B. Spectral Unmixing

It is well known that remotely sensed images often suffer serious mixture effects stemming from low spatial resolution, multiple scattering, and microscopic material mixing [34], [35]. Hyperspectral images are no exception. This discourages precise quantitative applications of hyperspectral imagery. Therefore, unmixing is desirable to promote efficient use of hyperspectral data. In contrast to multispectral data, hyperspectral data have unique advantages in the spectral unmixing thanks to the availability of many narrow, contiguous spectral bands for each pixel in a scene, which enables the extraction of more, finer endmembers (spectral signatures). Unmixing aims to accurately estimate the number of endmembers linked to individual constituent materials present in each pixel [23]. Generally, mixing models can be divided into two categories: the linear mixing model (LMM) and the nonlinear mixing model (NMM) [22]. The NMM assumes that interactions between the light scattered by multiple materials in the scene occur, while the LMM assumes no interactions between materials (i.e., no multiple scattering). According to the concepts, the LMM and NMM can be expressed as (1) and (2) respectively [36].

$$\rho_{\mathrm{mix}} = \sum_{i=1}^{N} f_i * \rho_i + \varepsilon \tag{1}$$

$$\rho_{\mathrm{mix}} = \sum_{i=1}^{N} f_i * \rho_i + \sum_{i=1}^{N}\sum_{j=1}^{N} f_{ij} * \rho_{ij} + \varepsilon \tag{2}$$

In (1) and (2), ρ_{mix} is the mixture reflectance measured by remote sensors, ρ_i is the endmember reflectance and f_i is the corresponding fraction (abundance) within a pixel. N is the number of endmembers for each pixel. ε denotes the model residual error resulting from random noise. Actually, it is far from sufficient to describe the NMM using (2) due to that the NMM usually results in an infinite sequence of powers of products of reflectance [34]. Here we aim to show the basic conceptual model of NMM, thus only the second-order mixture effect (ρ_{ij}), is considered in (2). Generally, the contributions of non-linear mixture items decrease with an increasing order. To keep the physical meanings of parameters in the above equations, the abundances of endmembers f_i and f_{ij} should be constrained by (3) and (4).

$$\sum_{i=1}^{N} f_i = 1$$
$$0 \le \mathrm{f}_i \le 1, \quad i = 1, 2, \ldots \mathrm{N} \tag{3}$$

$$\sum_{i=1}^{N} f_i + \sum_{i=1}^{N}\sum_{j=1}^{N} f_{ij} = 1$$
$$0 \le f_i, f_{ij} \le 1, \quad \mathrm{i,j} = 1, 2, \ldots \mathrm{N} \tag{4}$$

In general, the NMM is superior to the LMM in most cases because it describes the actual interactions at the Earth's surface. Neural networks have been confirmed as an effective way to extract endmembers using the NMM and associated abundances in each pixel [37], [38]. Recently, many improved neural network-based nonlinear unmixing algorithms such as the fuzzy ARTMAP neural network [39] have also been reported. Such studies have demonstrated that the improved methods are far better than conventional artificial neural networks and linear algorithms. The NMM can achieve higher estimation accuracy than the LMM, but it is more complicated. To resolve the problem, Wu *et al.* proposed a new hyperspectral unmixing algorithm based on a kernel orthogonal subspace projection. The new algorithm was found to outperform the support vector regression and radial basis function neutral network methods [40].

Although many researchers have turned their attention to the NMM and its applications, the LMM still holds an important role in the hyperspectral unmixing field because it is simple and effective in most cases. Like the NMM, the main tasks for linear spectral unmixing include endmember determination and abundance estimation. Since the method was first developed, considerable attention has focused on the first key step: endmember determination. Various algorithms have been developed, including iterative error analysis (IEA), vertex component analysis (VCA), the simplex growing algorithm (SGA), and minimum volume transform (MVT), which are mainly based on convex geometry characteristics [41]–[44]. Recently, many improvements in these algorithms have been made by Chinese researchers. Inspired by the IEA approach, Li *et al.* developed the hybrid endmember extraction algorithm (HEEA) [45]. Liu *et al.* proposed a new maximum simplex volume method based on the Householder transformation (HT) called the MVHT [46]. This method reduced computational complexity and provided consistent results, and thus outperformed both the VCA and SGA. Violating the pure-pixel assumption, Chan *et al.* presented a minimum-volume enclosing simplex (MVES) formulation for hyperspectral unmixing [47]. In addition, combinations of advanced mathematical optimization methods and biological theories for endmember extraction have been widely employed. For example, particle swarm optimization (PSO) and ant colony optimization (ACO) were successfully adopted to determine the endmembers by Zhang *et al.* [48], [49].

Hyperspectral imaging provides abundant spatial and spectral information on objects. Spatial information has become increasingly important in hyperspectral unmixing [50]–[52]. The integration of spectral and spatial information for hyperspectral unmixing has also been reported [53].

The final objective of hyperspectral unmixing is to estimate the abundance of each constituent (endmember) using the determined endmembers from each mixed pixel. In addition to the commonly used least-squares method, some numerical methods have also been proposed to estimate the proportion of each endmember in one pixel. These include independent component analysis (ICA) [54], non-negative matrix factorization (NMF) [55], and sparse regression-based unmixing [56]. These algorithms have made significant contributions to the abundance inversion, but they cannot be applied under all conditions because of certain defects. For example, the constrained ICA (cICA) experiences stability problems and the NMF is constrained to non-unique solutions. To overcome the shortcomings of these algorithms, numerous improvements have been developed in China, such as the improved-cICA [57], [58], the minimum volume constrained NMF (MVC-NMF) [59], and the smoothness- and sparseness-constrained NMF [60].

Traditional spectral unmixing techniques cannot obtain the spatial distribution of different compositions, only their exact abundances in a pixel. The exact spatial distributions of all the endmembers in a pixel are vital in precise quantitative hyperspectral remote-sensing applications. In 1997, Atkinson first proposed the concept of sub-pixel positioning. He noted that it was possible to assign the fractions spatially to "sub-pixels" [37]. Since then, increasing attention has been paid to a novel technique termed sub-pixel mapping [61]–[66]. The emerging technique is an extension of traditional hyperspectral unmixing and may ultimately overcome the resolution limitation of hyperspectral images.

C. Data Fusion and Super-Resolution Reconstruction

Hyperspectral imaging is often subject to low spatial resolution constraints. For example, the Chinese HJ-1A HSI has a ground resolution of about 100 m. To enhance the spatial resolution of airborne/satellite hyperspectral data, data fusion and super-resolution reconstruction techniques are of critical importance. Fusion of hyperspectral and multispectral images has become a hot topic. The aim is to incorporate the fine spatial context of multispectral images into hyperspectral images. Because of the special characteristics of hyperspectral images, conventional fusion methods such as the PCA-based fusion algorithm cannot be applied to hyperspectral image fusion directly. Instead, the wavelet-based fusion algorithm works well, as confirmed by Zhang *et al.* [67]. Another effective fusion strategy is based on hyperspectral unmixing [28]. Gu *et al.* proposed such a method to enhance the spatial resolution of hyperspectral images using spectral unmixing and super-resolution mapping techniques [68]. This type of method can perfectly fuse both spatial and spectral information. More important, the spectral unmixing-based algorithm is independent of the a priori information associated with the original data. Recently, a similarity-measure-based variational method was proposed by Shi *et al.*; this method completes the hyperspectral image fusion process [69] by transforming the problem into one of optimization using the variational model. It was shown to achieve good fusion results.

Super-resolution reconstruction is another important strategy to improve the ground resolution of hyperspectral imaging by data processing methods [70]. However, it is a challenging method. Until now, little research on super-resolution reconstruction of hyperspectral imaging has been reported in China.

D. Feature Selection and Extraction

Hyperspectral sensors image objects of interest in hundreds of narrow bands that form the spectral feature space of hyperspectral data. However, the original spectral features often contain high redundancy. The high-dimensional nature and strong

spectral correlation of hyperspectral data pose critical limitations in target discrimination and image classification. Not all bands from a hyperspectral image make the same contributions in applications. To overcome the dimensionality curse of hyperspectral data, it is desirable to reduce the original spectral feature space via feature selection and extraction [71], [72].

Over the past few decades, several research groups have sought to find an effective technique to construct a new feature space of lower dimensionality that retains the necessary information for specific applications. Zhao *et al.* [73] proposed a band-subset technology to improve the classification accuracy of hyperspectral imagery. Huang *et al.* [74] also worked on a new feature weighting method for band selection with a pairwise separability criterion and matrix coefficient analysis. Additionally, computational intelligence methods that rely on biological models (e.g., DNA, artificial immune systems, and neural networks) have been widely used for feature extraction and data analysis [75], [76]. Experimental results suggest that the computational intelligence method can yield better results than traditional algorithms for hyperspectral remote sensing imagery. However, these methods often require additional user-defined parameters to simulate the biological inversion process. This is a key factor that must be resolved in further work. In recent years, kernel methods, which mainly involve support vector machines (SVMs), kernel Fisher discriminant analysis, and a series of related kernel transformation techniques, have demonstrated excellent performance in hyperspectral data processing [77]–[79]. The properties of kernel methods make them well-suited to tackle the problem of information extraction because they can cope with large input spaces efficiently, thus avoiding the well-known Hughes phenomenon. Three commonly used kernel functions including polynomial kernel function, Gaussian kernel function and sigmoid kernel function are described as follows [80].

Polynomial kernel function:

$$K(x_\alpha, x_\beta) = [a(x_\alpha \cdot x_\beta) + b]^d \tag{5}$$

Gaussian kernel function:

$$K(x_\alpha, x_\beta) = \exp\left[-\frac{\|x_\alpha - x_\beta\|^2}{\delta}\right] \tag{6}$$

Sigmoid kernel function:

$$K(x_\alpha, x_\beta) = \tanh[-b(x_\alpha \cdot x_\beta) - c] \tag{7}$$

where a, b, c, and d are user-defined parameters. x_α and x_β are training or test samples, δ in (6) is the standard deviation of the Gaussian function.

Recently, increased attention has turned to the use of images with both high spatial and spectral resolution [77]. Such data provide detailed structural and spectral information, which make them more suitable for information extraction. In principle, feature extraction should use both the spectral information and the spatial relationship between pixels. Huang and Zhang [81], [82] proposed a spectral-spatial vector stacking method that included the pixel shape index (PSI) and gray level co-occurrence matrix (GLCM). Both of these indices exploit the structural and shape information in the images

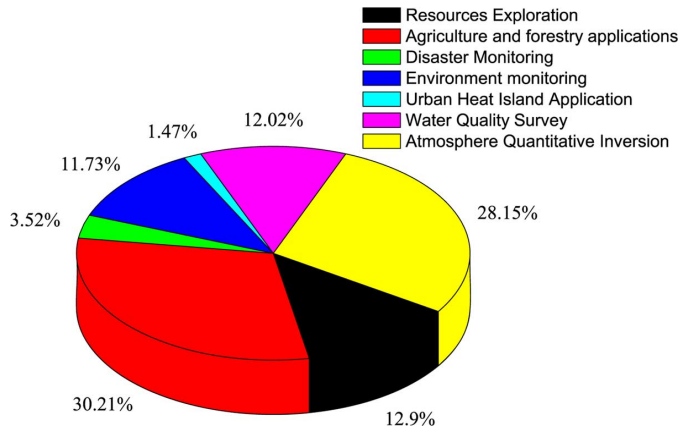

Fig. 12. Distribution of the main HRS application domains in China.

to complement the spectral feature space. In addition, the object-oriented approach is another effective way to extract subspace features. This method takes the spatial and contextual information into account for segmentation. The basic idea of object-based analysis (OBA) is to group spatially adjacent pixels into spectrally homogeneous objects and then classify each object as a minimum processing unit. The first and critical step of OBA is to accurately extract various objects in a scene by segmentation methods. To accomplish the goal, the commercial software eCognition developed by Definiens Imaging has incorporated an advanced segmentation approach termed Fractal Net Evolution (FNE) [83]. When performing FNE, a merge criterion for two adjacent objects is considered based on (8).

$$h = w * h_{\text{spectral}} + (1 - w) * h_{\text{spatial}}, \quad 0 \le w \le 1 \tag{8}$$

where w is the user-defined weight for spectral information, and h_{spectral} and h_{spatial} are respectively the spectral and spatial heterogeneities, and h is the overall merging criterion. Because of the effectiveness of OBA, many researchers have begun to use it in HRS data extraction [83]–[85].

IV. Typical Applications of Hyperspectral Imaging

The applications of HRS meet Chinese demands for resource exploration, environment monitoring, and land utilization. For historical reasons, economic and technological development in China was not regular until the 1980s. Since that time, the economy has grown rapidly and exploration of mineral resources is vital. This need provided initial development opportunities for HRS. After successful applications in resource exploration, HRS was also used in agriculture and forestry, which are two of the most important industries for any country.

Rapid economic growth has had negative effects on the environment. HRS has been used to monitor the environment, including water and atmospheric pollution and the effects of urban heat islands. China also experiences frequent natural disasters, and HRS has been widely used in disaster monitoring. Research on the biochemical parameters of vegetation using HRS has also been performed in China. Fig. 12 shows the main applications of HRS in China. According to Fig. 12, agriculture and forestry account for 30% of total HRS usage, making these the most important research topics related to HRS applications in China.

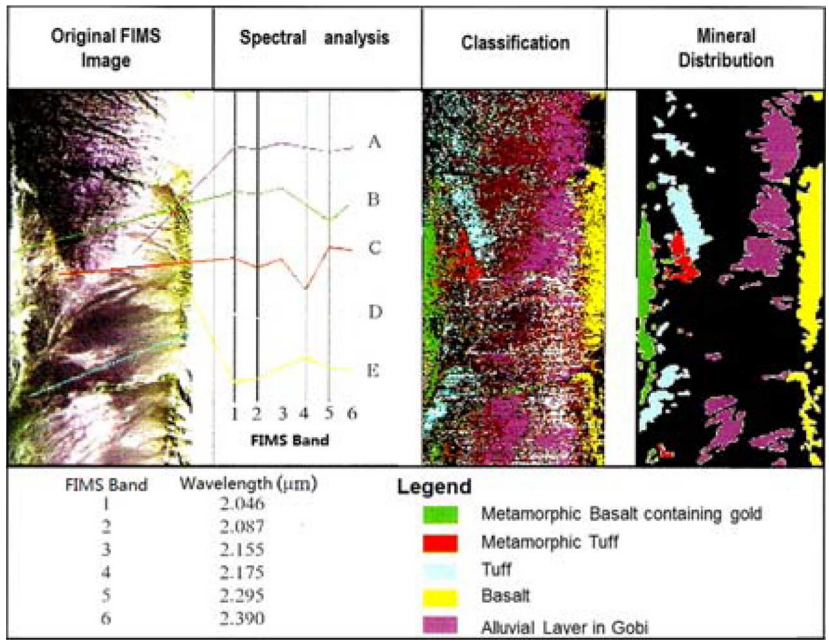

Fig. 13. Gold Exploration by FIMS in Xinjiang Province, China.

In the following section, some typical applications of HRS are discussed.

A. Mineral and Energy Resource Exploration

The first great achievement of HRS in China was in gold exploration in the 1980s in Xinjiang Province (Fig. 13). This research was based on a shortwave Fine-split Infrared Multispectral Scanner called FIMS [86], which, featuring 12 spectral bands within shortwave infrared wavelength range from 2.0 to 2.5 μm, is the first model of high spectral resolution imaging system developed by SITP, CAS. Tong *et al.* discovered some potential gold deposits areas, which were validated by a field survey, by modeling the gold spectral absorption index [87].

With the growth of mineral and energy exploration applications in HRS in recent decades, a series of new results has emerged from aerospace, aviation, ground, and core hyperspectral data [88]–[94]. Bi *et al.* used Hyperion data for the ZhongYang Mountains in East Kunlun, Qinghai-Tibet Plateau, to map altered minerals [95]. We also conducted an international cooperation with Australia to successfully extract uranium deposit information using MAIS data in the Pine Creek area of Australian in the 1990s as shown in Fig. 14. The uranium deposit information (The yellow color in Fig. 14) represents the uranium deposit extracted by using the Spectral Absorption Index of wavelength 2.114–2.147 μm and 2.336–2.367 μm from MAIS data showed a high consistency with validation results by both field survey and mineral geological map of Pine Creek. Liu *et al.* applied the CASI/SASI hyperspectral imaging system in uranium exploration. Good results were achieved in the extraction of alteration mineral information related to uranium mineralization on a large scale in the Keping region [96]. From June 2005 to June 2006, a study of oil and gas exploration was performed in Qinghai province, China, using Hyperion data [97].

China has also made progress in mineral exploration of the lunar surface using space hyperspectral data. Wu *et al.* showed

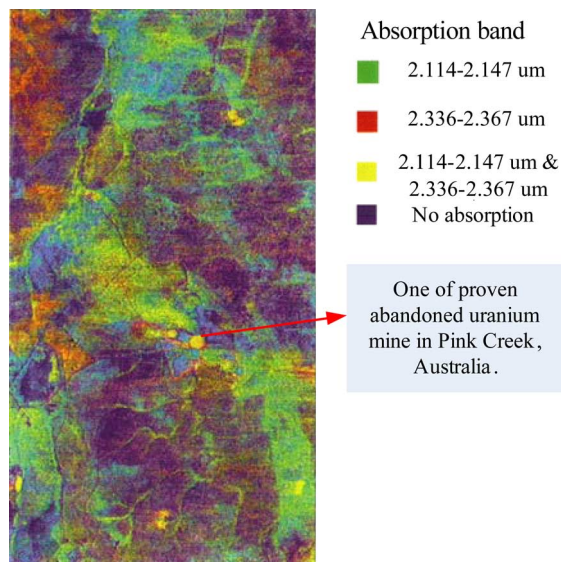

Fig. 14. Pine Creek Uranium mine investigation by MAIS data. The yellow color represents the uranium deposit extracted by using the Spectral Absorption Index with data in wavelength 2.114–2.147 μm and 2.336–2.367 μm.

the global distribution of compounds and minerals such as iron monoxide, titanium dioxide, orthopyroxene, clinopyroxene, olivine, and even plagioclase feldspar using data from the Chang'E-1 Interference Imaging Spectrometer [98], [99].

Although much progress has been made in HRS prospecting, China has not fully resolved the problem of meeting needs for rapid and deep mineral prospecting. This is a worldwide problem. Therefore we put forward a plan called the Spectral Crust project [100] which aims to combine imaging spectrometry, 3D visualization, data fusion, data assimilation, geology modeling, and other related technologies (e.g., geophysical and geochemical exploration) to map mineral and energy resources ranging from the Earth's surface to 1 km depth in China. The objective of the Chinese Spectral Crust project is very similar

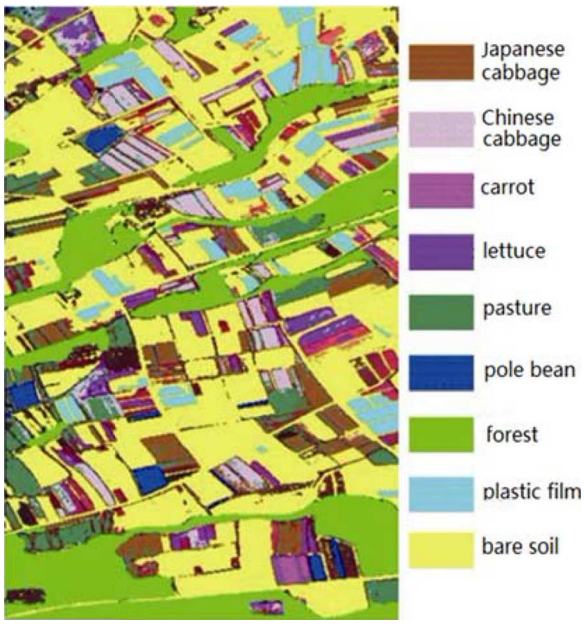

Fig. 15. Fine classification of vegetable-growing regions with PHI hyperspectral data.

to the Australia's "The Glass Earth" proposed in 1999, which focuses on making "transparent" the top 1000 m of the Earth's crust [101]. Remote sensing of alteration minerals and the development of an integrated aerospace, aerial, surficial, and below-ground core-based stereo detection system is also a priority of this project.

B. Agriculture and Forestry Applications

HRS applications in agriculture and forestry have developed quickly in recent decades [102]–[104]. Using hyperspectral data to monitor agricultural disasters can save time and money. Using PHI hyperspectral images, Yang *et al.* built a spectral information sounding and detection model of crop disease to identify wheat with stripe rust [105]. Tian *et al.* simplified the model of winter wheat drought by putting forward the notion of apparent thermal inertia (ATI) to replace real thermal inertia (RTI), which was previously widely used [106]. Other diverse studies of water content and stresses such as stripe rust have been reported by Liu *et al.* [107], [108] and Wang *et al.* [109]. Crop growth monitoring has made it possible to forecast production. Using a novel spectral index, Liu *et al.* improved winter wheat yield prediction [110]. The technology of fine classification in agriculture has matured greatly (Fig. 15).

Hyperspectral imaging has enabled the identification of tree species based on their contiguous spectra. One classic example is the experimental identification of six conifer species by Gong *et al.* [111]. Hyperspectral remote sensing has great potential for the accurate retrieval of forest biochemical parameters. Combining the geometrical-optical model 4-Scale and the modified leaf optical model PROSPECT, Zhang *et al.* estimated the leaf chlorophyll content from CASI imagery. They then estimated forest canopy reflectance using the measured leaf reflectance and transmittance spectra [112]. Zhao *et al.* proposed the normalization difference thermal index (NDTI) to monitor forest fires based on MODIS infrared radiation data. This approach was shown to be at least twice as fast as the fire monitoring algorithm model [113].

C. Environment Monitoring

The environmental problems caused by human activities have aroused widespread concern. Mine monitoring is one example of an environmental application of HRS. Gan *et al.* used Hyperion data to detect pollutants from the Dexing copper mine in Jiangxi Province [114]. Zhang *et al.* successfully employed a vegetation inferiority index (VII) and water absorption disrelated index (WDI) to monitor the vegetation and environment in the mining area [115]. However, the most serious and widespread environmental problems involve water and atmospheric pollution and the effects of urban heat islands, caused by rapid economic development and urbanization.

1) Water Resources Monitoring: In recent years, the government of China has devoted much energy to monitoring polluted water (lakes and rivers). Yan *et al.* established an empirical inversion model for chlorophyll and suspended substances using Hyperion satellite-borne hyperspectral remote sensor data and data from 25 synchronous water sampling points [116]. This model was found to have high enough precision to allow monitoring of the water quality of Taihu Lake. Zhou *et al.* obtained an optimized multi-spectral combination that is closely related to chlorophyll concentration but little influenced by suspended material [117]. This method effectively retrieved the chlorophyll-a concentration in highly turbid, hyper-eutrophic inland waters. Sun *et al.* used hyperspectral data to estimate the chlorophyll-a in Lake Taihu. They found the SVM algorithm to be robust for remotely estimating chlorophyll-a in inland turbid lake waters [118]. For the next generation of water color hyperspectral sensors, Shen *et al.* performed Level-1 requirements in different spectra that could capture the spectral curve of inland water and also avoid band wastage for data storing and memory [119]. To design a robust hyperspectral remote sensing-based water resources monitoring system in China, we put efforts to the research on related key technologies using hyperspectral images in 2006. This was systematically introduced by Hu *et al.* [120]. On this basis, suspended matter concentrations of Meiliang Bay of Taihu Lake were estimated using the CHRIS data by Li as presented in Fig. 16 [121].

2) Air Quality Assessment: Hyperspectral remote sensing plays an important role in detection of greenhouse gases (e.g., CO, CH4, and CO2), pollutants (e.g., NO2, SO2, and HCHO), clouds, and aerosols. To detect these compounds, some hyperspectral satellite detectors have been launched, such as SCIAMACHY, AIRS, GOSAT, and MODIS. In China, research on the inversion of atmospheric trace constituents with hyperspectral data began only a few years ago. With the improvement of living standards, more attention is being paid to pollution and greenhouse gases [122], [123]. Jiang *et al.* researched long-term SO2 concentrations using the Ozone Monitoring Instrument (OMI) and found that they had an imbalanced spatial distribution, with the highest level in central East China [124] (Fig. 17). Wang *et al.* observed the spatial and temporal variations in CO2 over China using SCIAMACHY

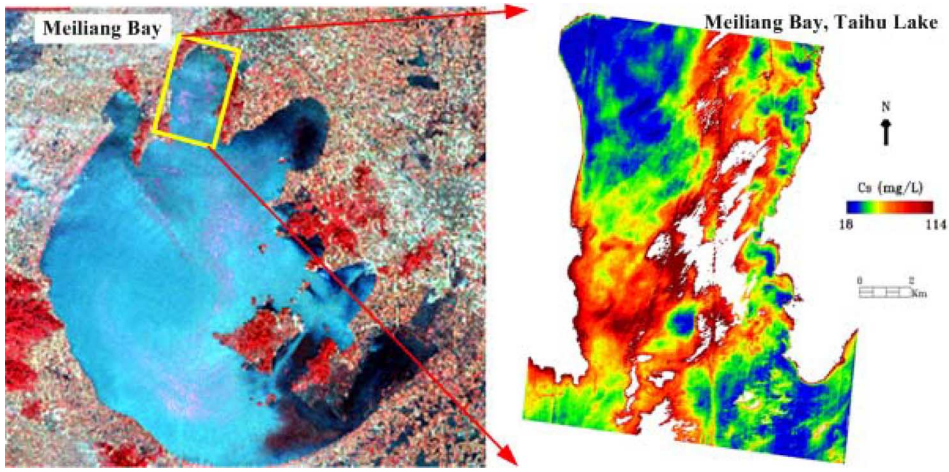

Fig. 16. Distribution of the suspended matter concentration Meiliang Bay of Taihu Lake. Left: LANDSAT TM image of Taihu Lake; Right: suspended matter estimation result of Meiliang Bay by CHRIS data.

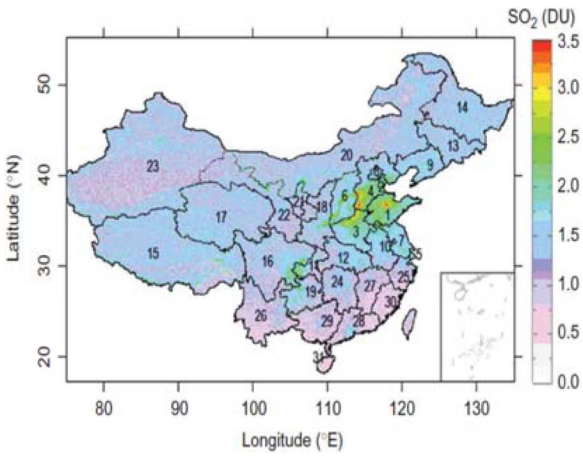

Fig. 17. Distribution of the average planetary boundary layer SO2 column concentration over China during 2005–2008. 1, Shandong; 2, Tianjin; 3, Henan; 4, Hebei; 5, Shanghai; 6, Shanxi; 7, Jiangsu; 8, Beijing; 9, Liaoning; 10, Anhui; 11, Chongqing; 12, Hubei; 13, Jilin; 14, Heilongjiang; 15, Xizang (Tibet); 16, Sichuan; 17, Qinghai; 18, Shaanxi; 19, Guizhou; 20, Neimenggu; 21, Ningxia; 22, Gansu; 23, Xinjiang; 24, Hunan; 25, Zhejiang; 26, Yunnan; 27, Jiangxi; 28, Guangdong; 29, Guangxi; 30, Fujian; 31, Hainan.

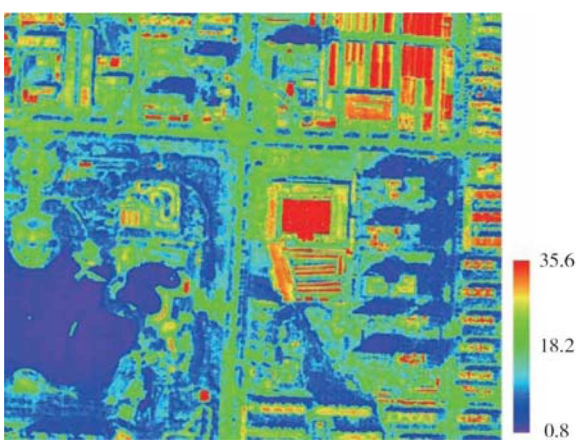

Fig. 18. Distribution of the diurnal temperature of the land surface in Shijiazhuang, China.

satellite data [125]. Their results showed obvious spatial variations of the CO2 concentration in the whole of China, with clear seasonal fluctuation during 2003–2005.

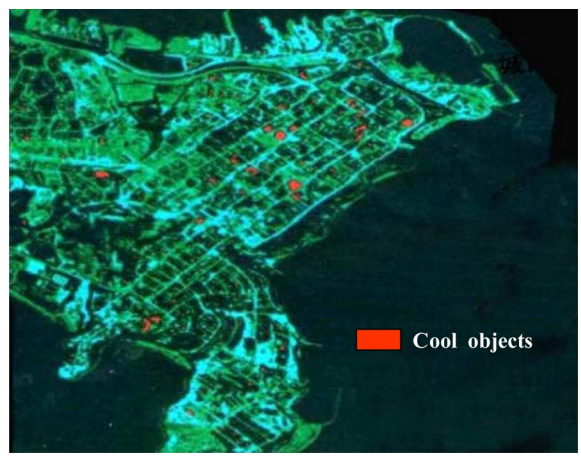

Fig. 19. Monitoring of cold energy leaks in Darwin, Australia using TIR wavelength bands data of MAIS sensor.

To study aerosols, Wang *et al.* used the vertical and relative humidity (RH) correcting method to retrieve aerosol optical thickness (AOT) and the surface-level particulate matter (PM) concentrations with MODIS data and ground-based measurements [126]. The study showed that MODIS data can be used to monitor the regional air pollution via the vertical and RH correcting method.

3) Study on Urban Environment: Urban environment has been seriously impacted by human's social and economic activities. With the rapid urbanization of China, the effect of urban heat islands has increased, which makes the temperature in cities higher than that in nearby rural areas. Surface temperature and reflectivity inversion are key challenges for urban heat island monitoring. In 2008, Xu *et al.* used airborne hyperspectral imagery data (OMIS) to model the sensible heat flux from Shanghai on multiple spatial scales. They suggested that using much lower spatial resolution, spaceborne image data is a practical solution for heat flux determination [127]. The IRSA, CAS performed synchronization trials for hyperspectral thermal infrared imagery obtained by TASI and field measurements in Shi Jiazhuang, Hebei province, from July to August 2010. As part of this trial, Yang *et al.* accurately isolated the surface temperature and emissivity based on TASI data [128]

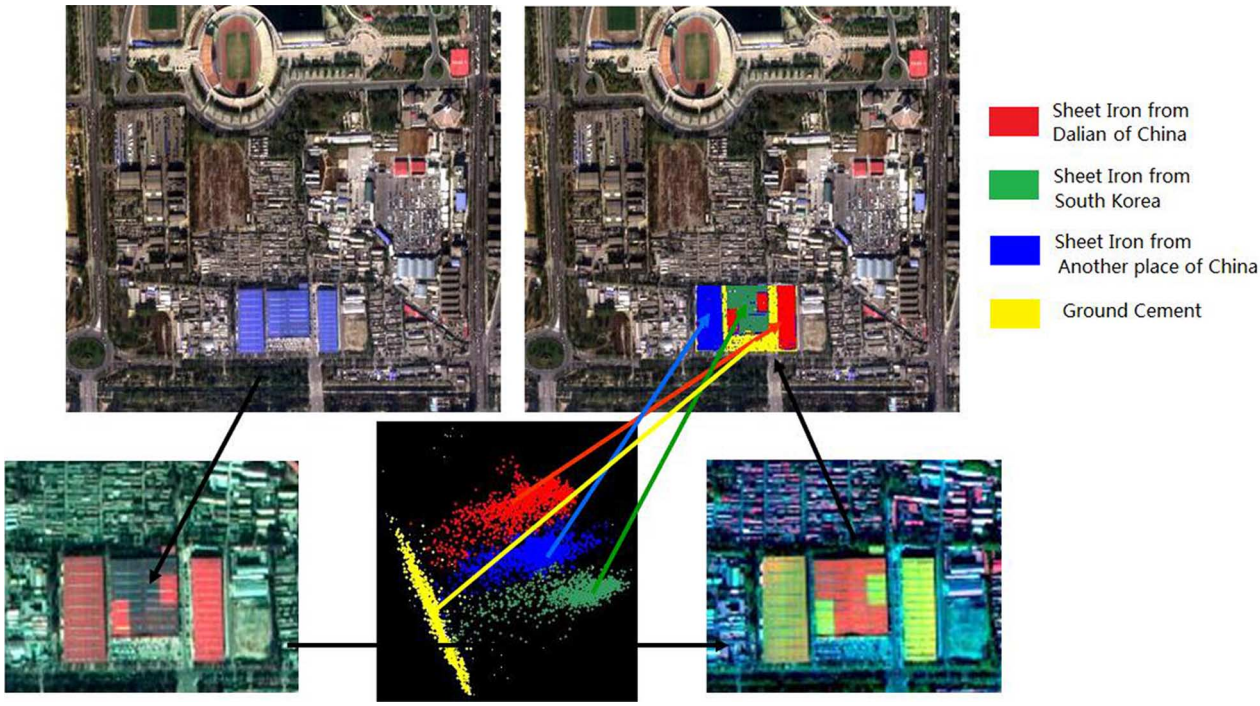

Fig. 20. Identification of roof sheet iron using the OMIS-II hyperspectral imagery.

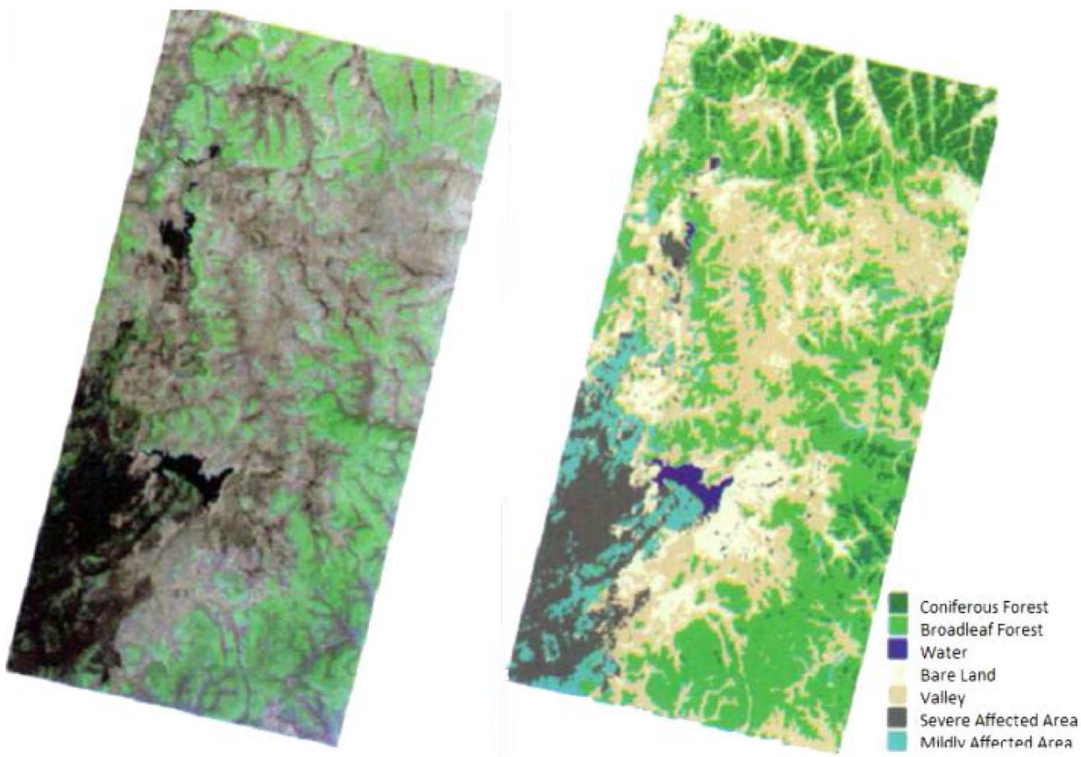

Fig. 21. Vegetation recovery monitoring after a fire using HJ-1A HSI data.

(Fig. 18). Yang *et al.* also analyzed the influence of spectral resolution on the precision of the temperature retrieval. They found that when the spectral resolution is about 0.172 μm it yields the highest estimation accuracy and the research results may contribute to the development of future thermal infrared hyperspectral sensors [129]. As well as monitoring urban heat islands, we were also invited to monitor the urban energy waste in Darwin city of Australia using the MAIS onboard the Citation S/II aircraft in the 1990s. The successful experiment was reported as "Hi-tech check shows energy waste in city" by Australia News in 1991. Fig. 19 shows the cool objects (red color) due to cold energy leaking from roofs of air-conditioned rooms. The cool objects (with lower temperatures compared with the surroundings) were calculated by performing a band

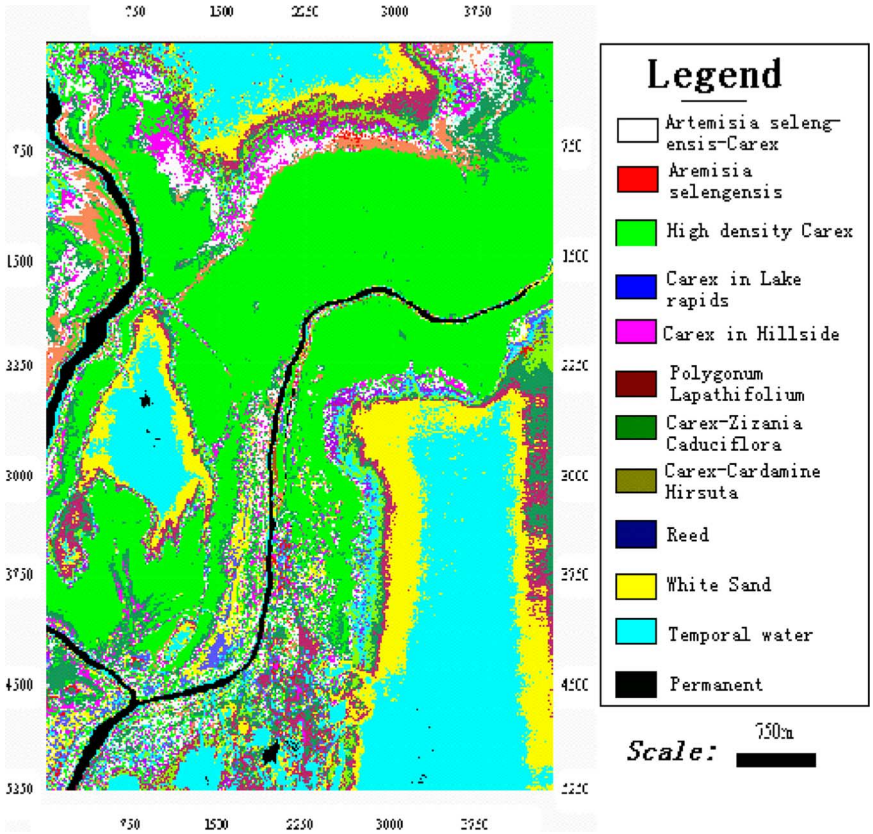

Fig. 22. Classification of wetland vegetation by spectral matching technique in Poyang Lake area.

math function using TIR wavelength bands data of MAIS sensor.

In addition to monitoring of the urban heat island effect, other typical applications related to urban environment with HRS have been also carried out over the past decades. These included the identification of roof sheet iron manufactured by different corporations surrounding the Beijing Asian Games village [130]. As shown in Fig. 20, it is hard to tell apart the blue iron sheets separately from Dalian of China, South Korea and another Chinese corporation with the visible wavelengths of OMIS-II hyperspectral imagery. However, they are clearly distinguished from each other by the convex geometry projection transform due to taking full advantages of high-dimensional property of hyperspectral remote sensing.

D. Disaster Monitoring

Hyperspectral imaging can also be used to monitor natural disasters, such as droughts, floods, fires, snows, earthquakes, dust storms, and typhoons. The Environment and Disaster Monitoring Microsatellite HJ-1A has provided hyperspectral data for early warning, monitoring, assessment, and analysis in natural disasters [131].

HRS has been widely used in China for pre-disaster early warning and monitoring. Cui *et al.* used the hyperspectral sensor AIRS to retrieve the amount of water vapor, CO, and CH4 in the Yushu area, finding that the amount of CO increased before an earthquake. This knowledge could play an important role in earthquake prediction [132].

In regard to dynamic disaster monitoring, hyperspectral applications mainly focus on droughts and soil and marine disasters. Pang *et al.* used MODIS and meteorological data to establish a drought monitoring model based on the vegetation supply water index algorithm (VSWI) [133]. Weng *et al.* extracted information on saline soil semi-quantitatively using its spectral characteristics [134].

In post-disaster assessment and analysis, the advantage of hyperspectral methods lies in their rapid assessment of damage. This was the case for a snow disaster in southern China in 2008. There, the infrared channels of MODIS were used for surface temperature inversion and compared to the data of 2007, in order to assess loss on the third day after the disaster [135]. Furthermore, the HSI data of HJ-1A were used to calculate the leaf area index and retrieve chlorophyll content for monitoring of forest regrowth after a fire (Fig. 21) [136].

E. Vegetation Information Extraction

Biochemical parameters are important for research on vegetation growth, the carbon cycle, and global climate change. Research on biochemical parameter inversion of vegetation in China has received growing attention in recent years. Gross primary production (GPP) is a critical variable in the global carbon cycle [137]. Wu *et al.* found a close relationship between chlorophyll content and light use efficiency (LUE) in data for wheat obtained using an ASD (analytical spectral device). They then achieved remote retrieval of the GPP [138]. Wu next performed

TABLE IX
HYPERSPECTRAL DATA PROCESSING SYSTEMS AND COUNTRY OF DEVELOPMENT

Name	Developer	Country
HIPAS	Institute of Remote Sensing Application, Chinese Academy of Sciences	China
ISDPS	China Areo Geophysical Survey & Remote Sensing Center for Land and Resources	China
SPAM	The Spectral Analysis Manager-JPL	United States
ISIS	Integrated Software for Imaging Spectrometers -USGS Flagstaff	United States
HIPS	Hyperspectral Image Processing System	United States
SIPS	The Spectral Image Processing System -University of Colorado	United States
HYDICE	The HYDICE Starter Kit -Naval Research Lab	United States
Genisis	General Imaging Spectrometry Interpretation System-WTJ systems	United States
MIDAS	MIDAS-TASC	United States
ENVI	The Environment for Visualizing Images, Research Systems Inc.	United States
ERDAS	ERDAS-Hyperspectral Data Analysis Package	United States
TETRACORDER	U.S. Geological Survey	United States
ISDAS	Imaging Spectrometer Data Analysis System-CCRS	Canada
PCI	PCI-ERDAS-Hyperspectral Data Analysis Package	Canada
The Spectral Geologist	Commonwealth Scientific and Industrial Research Organization(CSIRO)	Australia

a series of studies on GPP [139]–[143]. Shen *et al.* [144] estimated the aboveground biomass for five major grassland ecosystems on the Tibetan Plateau using the vegetation index based on universal pattern decomposition (VIUPD) [145], which showed the lowest prediction error among eight vegetation indices such as NDVI and EVI. The VIUPD first developed by Zhang *et al.* is expressed as a linear sum of the pattern decomposition coefficients and features sensor independence [146]. Since its development, the new vegetation index has been assessed and improved using different sensors to accurately extract vegetation information, thereby better estimate the NPP or GPP of the terrestrial vegetation [144], [147], [148]. The chlorophyll content and distribution in leaves is an important index in estimation of plant nutrition information [149], which is an important indicator of vegetation health. Research on chlorophyll inversion was widely performed in winter wheat [150], rice [151], [152], and cucumber [153].

The wetland is a sensitive indicator of the global and regional environment and thus its investigations have been also emphasized in China. In 1997, a cooperation project between the National Remote Sensing Center of China and the National Space development Agency of Japan was conducted using the MAIS and PHI to estimate vegetation biomass of the wetland in Poyang Lake area, China. Comparisons between vegetation biomass derived by the HRS technology and the ground truth yielded a high consistency. Fig. 22 illustrates a precise classification result of wetland vegetation in Poyang Lake region.

Due to the increasing demand for land and development, China's wetlands are rapidly disappearing. Recently, Niu *et al.* reported their research on China's natural wetlands based on statistics during the period of 1987–2008 in Nature [154]. Research found that 33% of the country's natural wetlands have disappeared since 1987, largely due to land reclamation that accounts for more than 70%. Therefore, they appealed that more protection for China's wetland are urgently needed. Hyperspectral remote sensing will play a more important role in this campaign of natural wetlands monitoring and protection.

V. DEVELOPMENT OF SOFTWARE AND TOOLS FOR HYPERSPECTRAL DATA

The popularity of hyperspectral remote sensing technology is closely tied to the development of hyperspectral image processing and analysis software and tools. As a result, special attention has been paid to designing, developing, and commercializing various generic or professional software and tools related to hyperspectral imaging across the HRS community. More than ten commercial hyperspectral data processing systems have been created worldwide, including ENVI by the Environment for Visualizing Images, Research System Inc. Table IX lists most of the systems developed to date.

The table includes two hyperspectral data processing systems developed in China (HIPAS and ISDPS). These were developed by IRSA, CAS, and by the China Aero-Geophysical Survey & Remote Sensing Center for Land and Resources, respectively. HIPAS (Hyperspectral Image Processing and Analysis System, see Fig. 23) [155], which was the first Chinese generic hyperspectral data processing system programmed in C++, can operate in a Windows environment without any strict configuration requirements. This makes it convenient for both professional researchers and general users. HIPAS can preprocess the original data obtained by the MAIS, PHI, and OMIS developed in China and can use popular hyperspectral imaging data from around the world. The main functions of HIPAS can be divided into seven modules: data input and output, data preprocessing, conventional image processing, spectral analysis, interactive analysis, spectral database management, and advanced features. Furthermore, HIPAS features a transplantable environment for new algorithms, which can be added to the system according to need. A spectral database constructed by FoxPro was also integrated

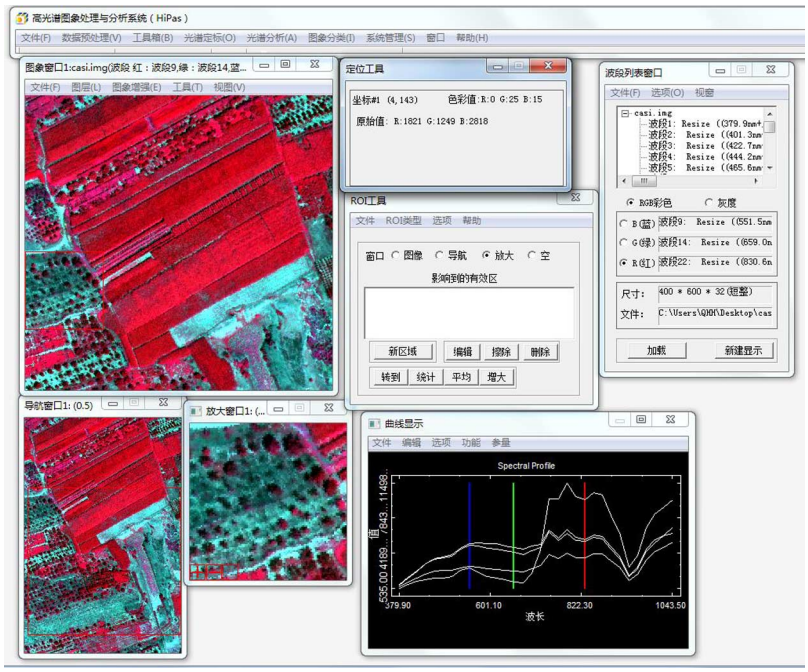

Fig. 23. The system interface of HIPAS.

into the HIPAS system. As a result, newly measured spectral data can be inputted and stored at any time. Since its distribution, HIPAS has been used in a number of applications including mineral identification, urban land-use investigation, and vegetation and crop classification.

In addition to the HIPAS and ISDPS hyperspectral data processing systems listed in the Table IX, many prototype software and tools have also been designed and developed in China to meet the increasing demands for hyperspectral data processing and analysis. These include the Remote-sensing Environmental Monitoring System (REMS) from IRSA, CAS [156], and WATERS, designed for monitoring of water quality and the environment by the Center for Earth Observation and Digital Earth, Chinese Academy of Sciences (CEODE, CAS). These tools can be mainly summarized into three categories: hyperspectral data acquisition system, hyperspectral data preprocessing system, and hyperspectral information extraction and analysis system. Fig. 24 presents statistics for HRS software or tool development since 2006 based on data from the Copyright Protection Center of China.

In addition, hyperspectral databases have been also emphasized for promoting the development of HRS in China during the last 30 years [157]. A standard remote sensing spectral database for typical surface features was successfully developed in 2005 by Beijing Normal University under the support of the National High Technology Research and Development Program of China (863 Program). The spectral database integrates various analytical models and computer simulations alongside measured spectral data (i.e., remotely sensed images for typical surface features), environmental factors, and a priori knowledge. Thus it has contributed greatly to quantitative remote sensing research in China.

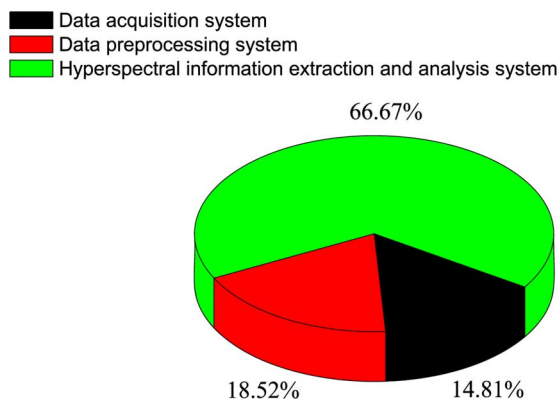

Fig. 24. Software or tools related to HRS developed in China since 2006.

More recently, Zhang *et al.* presented the concept of the multidimensional hyperspectral database for rocks and minerals [158]. This attempts to meet the increasing demands for new remote sensing spectral databases that can retrieve and analyze spectral data on multiple spatial and spectral scales for various purposes. A prototype database is being designed with support from the National Natural Science Foundation of China.

VI. Conclusions and Prospects

Hyperspectral remote sensing of the Earth and deep space is an appealing topic but also a challenging one. Since the 1980s, great attention has been paid to the development of hyperspectral imaging in various fields including agriculture, forestry, urban, natural and ocean environments, geology, and climate change. As Goetz expressed in his review of three decades of hyperspectral remote sensing of the Earth [3], the technique has experienced a long and difficult developmental process. Thanks to the great attention given by the Chinese

government and support from many major national programs, China has made significant achievements in this field during the past three decades. These range from hyperspectral remote sensing theories, to imaging mechanisms and sensors, to hyperspectral data processing and analysis techniques. The progress has enhanced the demand for applications in Earth exploration and environmental monitoring. With rapid advances in HRS technology and the launch of Chang'E-1 IIM under the China's Lunar Exploration Program (CLEP), the demand has been extended to deep space exploration with HRS, which will aid in understanding the environment beyond Earth.

This overview of the state of the art in HRS in China over the last 30 years clearly shows that encouraging achievements have been made. However, challenges and gaps with other countries still exist. Future exploration of HRS should focus on the development of high-performance hyperspectral remote sensors that feature high spatial/spectral resolutions and appropriate SNR levels, as well as investigations of key techniques. These include hyperspectral data mining, spectral unmixing, spectral matching, and multi-scale conversion. Another problem is that few software or tools for hyperspectral imaging have been successfully commercialized and distributed in China, which greatly discourages the development of HRS. To our delight, the Medium- to Long-Term Scientific and Technological Development Plan (2006–2020) lists the development of a high-resolution (high spatial, high spectral and high temporal resolutions) earth observation system as a major project. This plan will provide a good opportunity to resolve remaining problems and achieve new heights in the development of HRS in China.

ACKNOWLEDGMENT

The authors gratefully acknowledge Dr. Qian Du from the Department of Electrical and Computer Engineering, Geosystems Research Institute-High Performance Computing Collaboratory, Mississippi State University, for her encouragement on completing this manuscript. The authors give special thanks to Changping Huang, Hongxing Qi, Taixia Wu, Yi Cen, Tong Shuai, Hengqian Zhao, Kai Liu, Xuejian Sun, Xiaojun She, Xueke Li, Yao Li, Tingting Shi, and Guizhen Wang for their significant contributions to this paper.

REFERENCES

[1] A. F. H. Goetz, G. Vane, J. E. Solomon, and B. N. Rock, "Imaging spectrometry for earth remote-sensing," *Science*, vol. 228, pp. 1147–1153, 1985.

[2] A. F. H. Goetz, "Hyperspectral imaging and quantitative remote sensing," *Land Satellite Information in the Next Decade*, pp. E1–E10, 180, 1995.

[3] A. F. H. Goetz, "Three decades of hyperspectral remote sensing of the earth: A personal view," *Remote Sens. Environ.*, vol. 113, pp. S5–S16, 2009.

[4] C. Chang, *Hyperspectral Imaging: Techniques for Spectral Detection and Classification*. New York, NY, USA: Springer, 2003.

[5] K. L. Castro-Esau, G. A. Sanchez-Azofeifa, B. Rivard, S. J. Wright, and M. Quesada, "Variability in leaf optical properties of Mesoamerican trees and the potential for species classification," *Am. J. Botany*, vol. 93, pp. 517–530, Apr. 2006.

[6] Y. B. Cheng, S. L. Ustin, D. Riano, and V. C. Vanderbilt, "Water content estimation from hyperspectral images and MODIS indexes in Southeastern Arizona," *Remote Sens. Environ.*, vol. 112, pp. 363–374, Feb. 15, 2008.

[7] A. Plaza, J. A. Benediktsson, J. W. Boardman, J. Brazile, L. Bruzzone, G. Camps-Valls, J. Chanussot, M. Fauvel, P. Gamba, A. Gualtieri, M. Marconcini, J. C. Tilton, and G. Trianni, "Recent advances in techniques for hyperspectral image processing," *Remote Sens. Environ.*, vol. 113, pp. S110–S122, Sep. 2009.

[8] Q. Tong, Y. Xue, J. Wang, L. Zhang, J. Fang, Y. Yang, X. Liu, H. Qi, L. Zheng, and C. Huang, "Development and application of the field imaging spectrometer system," *J. Remote Sens.*, vol. 14, pp. 409–422, 2010.

[9] L. Zhang, C. Huang, T. Wu, F. Zhang, and Q. Tong, "Laboratory calibration of a field imaging spectrometer system," *Sensors*, vol. 11, pp. 2408–2425, 2011.

[10] J. Wang and Y. Xue, "Airborne imaging spectrometers developed in China," in *SPIE*, Beijing, China, 1998.

[11] B. Liu, J. Y. Fang, X. Liu, L. F. Zhang, B. Zhang, and Q. X. Tong, "Research on crop-weed discrimination using a field imaging spectrometer," *Spectroscopy and Spectral Analysis*, vol. 30, pp. 1830–1833, Jul. 2010.

[12] C. Huang, L. Zhang, X. Zhang, L. Zheng, and Q. Tong, "Study on discrimination of varieties of milk based on FISS imaging spectral data," *Spectroscopy and Spectral Analysis*, vol. 31, pp. 214–218, Jan. 2011.

[13] C. Huang, L. Zhang, J. Fang, and Q. Tong, "A radiometric calibration model for the field imaging spectrometer system," *IEEE Trans. Geosci. Remote Sens.*, vol. 51, pp. 2465–2475, 2013.

[14] J. S. Pearlman, P. S. Barry, C. C. Segal, J. Shepanski, D. Beiso, and S. L. Carman, "Hyperion, a space-based imaging spectrometer," *IEEE Trans. Geosci. Remote Sens.*, vol. 41, pp. 1160–1173, 2003.

[15] Z. Mao, J. Chen, and X. He, "Evaluation of CMODIS-measured radiance by a hyperspectral model," *Int. J. Remote Sens.*, vol. 31, pp. 5179–5198, 2010.

[16] Y. Wu, B. Xue, B. Zhao, P. Lucey, J. Chen, X. Xu, C. Li, and Z. Ouyang, "Global estimates of lunar iron and titanium contents from the Chang'E-1 IIM data," *J. Geophys. Res.*, vol. 117, 2012.

[17] A. Cheriyadat, "Limitations of principal component analysis for dimensionality-reduction for classification of hyperspectral data," Mississippi State University, MS, USA, pp. 31–56, 2003.

[18] F. A. Mianji and Y. Zhang, "Robust hyperspectral classification using relevance vector machine," *IEEE Trans. Geosci. Remote Sens.*, vol. 49, pp. 2100–2112, Jun. 2011.

[19] N. Acito, M. Diani, and G. Corsini, "Hyperspectral signal subspace identification in the presence of rare signal components," *IEEE Trans. Geosci. Remote Sens.*, vol. 48, pp. 1940–1954, Apr. 2010.

[20] Q. Tong, B. Zhang, and L. Zheng, *Hyperspectral Remote Sensing—Principles, Techniques and Applications*. Beijing, China: Higher Education Press, 2006.

[21] , C.-I. Chang, Ed., *Hyperspectral Data Exploitation: Theory and Applications*. New York, NY, USA: Wiley-Interscience, 2007.

[22] N. Keshava and J. F. Mustard, "Spectral unmixing," *IEEE Signal Process. Mag.*, vol. 19, pp. 44–57, 2002.

[23] C. Quintano, A. Fernández-Manso, Y. E. Shimabukuro, and G. Pereira, "Spectral unmixing," *Int. J. Remote Sens.*, vol. 33, 2012.

[24] T. A. Wilson, S. K. Rogers, and M. Kabrisky, "Perceptual-based image fusion for hyperspectral data," *IEEE Trans. Geosci. Remote Sens.*, vol. 35, pp. 1007–1017, Jul. 1997.

[25] M. T. Eismann and R. C. Hardie, "Application of the stochastic mixing model to hyperspectral resolution, enhancement," *IEEE Trans. Geosci. Remote Sens.*, vol. 42, pp. 1924–1933, Sep. 2004.

[26] R. C. Hardie, M. T. Eismann, and G. L. Wilson, "MAP estimation for hyperspectral image resolution enhancement using an auxiliary sensor," *IEEE Trans. Image Process.*, vol. 13, pp. 1174–1184, Sep. 2004.

[27] M. T. Eismann and R. C. Hardie, "Hyperspectral resolution enhancement using high-resolution multispectral imagery with arbitrary response functions," *IEEE Trans. Geosci. Remote Sens.*, vol. 43, pp. 455–465, Mar. 2005.

[28] N. Yokoya, T. Yairi, and A. Iwasaki, "Coupled nonnegative matrix factorization unmixing for hyperspectral and multispectral data fusion," *IEEE Trans. Geosci. Remote Sens.*, vol. 50, pp. 528–537, Feb. 2012.

[29] S. C. Park, M. K. Park, and M. G. Kang, "Super-resolution image reconstruction: A technical overview," *IEEE Signal Process. Mag.*, vol. 20, pp. 21–36, May 2003.

[30] Z. He and B. He, "Weight spectral angle mapper (WSAM) method for hyperspectral mineral mapping," *Spectroscopy and Spectral Analysis*, vol. 31, pp. 2200–2204, 2011.

[31] S. Fang and H. Gong, "Spectral similarity scale based on dynamic wighting adjustment method," *Geomatrics and Information Science of Wuhan University*, vol. 31, pp. 1044–1046, 2006.

[32] H. Jiao, Y. Zhong, and L. Zhang, "Artificial DNA computing-based spectral encoding and matching algorithm for hyperspectral remote sensing data," *IEEE Trans. Geosci. Remote Sens.*, vol. 50, pp. 4085–4104, 2012.

[33] P. Du, J. Xia, W. Zhang, K. Tan, Y. Liu, and S. Liu, "Multiple classifier system for remote sensing image classification: A review," *Sensors (Basel)*, vol. 12, pp. 4764–92, 2012.

[34] J. M. Bioucas-Dias, A. Plaza, N. Dobigeon, M. Parente, Q. Du, P. Gader, and J. Chanussot, "Hyperspectral unmixing overview: Geometrical, statistical, and sparse regression-based approaches," *IEEE J. Sel. Topics Appl. Earth Observ. Remote Sens.*, vol. 5, pp. 354–379, 2012.

[35] C. Small, "High spatial resolution spectral mixture analysis of urban reflectance," *Remote Sens. Environ.*, vol. 88, pp. 170–186, 2003.

[36] X. Chen and L. Vierling, "Spectral mixture analyses of hyperspectral data acquired using a tethered balloon," *Remote Sens. Environ.*, vol. 103, pp. 338–350, 2006.

[37] P. M. Atkinson, "Mapping sub-pixel boundaries from remotely sensed images," *Innovations in GIS*, vol. 4, pp. 166–180, 1997.

[38] K. J. Guilfoyle, M. L. Althouse, and C. I. Chang, "A quantitative and comparative analysis of linear and nonlinear spectral mixture models using radial basis function neural networks," *IEEE Trans. Geosci. Remote Sens.*, vol. 39, pp. 2314–2318, 2001.

[39] K. Wu, L. Zhang, and P. Li, "A neural network method of selective endmember for pixel unmixing," *J. Remote Sens.-Beijing*, vol. 11, p. 20, 2007.

[40] B. Wu, L. Zhang, P. Li, and J. Zhang, "Nonlinear estimation of hyperspectral mixture pixel proportion based on kernel orthogonal subspace projection," *Advances in Neural Networks–ISNN 2006*, pp. 1070–1075, 2006.

[41] C. I. Chang, C. C. Wu, W. Liu, and Y. C. Ouyang, "A new growing method for simplex-based endmember extraction algorithm," *IEEE Trans. Geosci. Remote Sens.*, vol. 44, pp. 2804–2819, 2006.

[42] M. D. Craig, "Minimum-volume transforms for remotely sensed data," *IEEE Trans. Geosci. Remote Sens.*, vol. 32, pp. 542–552, 1994.

[43] J. M. P. Nascimento and J. M. B. Dias, "Vertex component analysis: A fast algorithm to unmix hyperspectral data," *IEEE Trans. Geosci. Remote Sens.*, vol. 43, pp. 898–910, 2005.

[44] R. Neville, K. Staenz, T. Szeredi, J. Lefebvre, and P. Hauff, "Automatic endmember extraction from hyperspectral data for mineral exploration," in *Proc. 21st Canadian Symp. Remote Sens.*, 1999, pp. 21–24.

[45] H. Li and L. Zhang, "A hybrid automatic endmember extraction algorithm based on a local window," *IEEE Trans. Geosci. Remote Sens.*, vol. 49, pp. 4223–4238, 2011.

[46] J. M. Liu and J. S. Zhang, "A new maximum simplex volume method based on householder transformation for endmember extraction," *IEEE Trans. Geosci. Remote Sens.*, vol. 50, pp. 104–118, Jan. 2012.

[47] T. H. Chan, C. Y. Chi, Y. M. Huang, and W. K. Ma, "A convex analysis-based minimum-volume enclosing simplex algorithm for hyperspectral unmixing," *IEEE Trans. Signal Process.*, vol. 57, pp. 4418–4432, Nov. 2009.

[48] B. Zhang, X. Sun, L. Gao, and L. Yang, "Endmember extraction of hyperspectral remote sensing images based on the discrete particle swarm optimization algorithm," *IEEE Trans. Geosci. Remote Sens.*, vol. 49, pp. 4173–4176, 2011.

[49] B. Zhang, X. Sun, L. Gao, and L. Yang, "Endmember extraction of hyperspectral remote sensing images based on the ant colony optimization (ACO) algorithm," *IEEE Trans. Geosci. Remote Sens.*, vol. 49, pp. 2635–2646, 2011.

[50] G. Martín and A. Plaza, "Region-based spatial preprocessing for endmember extraction and spectral unmixing," *IEEE Geosci. Remote Sens. Lett.*, vol. 8, pp. 745–749, 2011.

[51] A. Plaza, P. Martínez, R. Pérez, and J. Plaza, "Spatial/spectral endmember extraction by multidimensional morphological operations," *IEEE Trans. Geosci. Remote Sens.*, vol. 40, pp. 2025–2041, 2002.

[52] D. Rogge, B. Rivard, J. Zhang, A. Sanchez, J. Harris, and J. Feng, "Integration of spatial-spectral information for the improved extraction of endmembers," *Remote Sens. Environ.*, vol. 110, pp. 287–303, 2007.

[53] S. Mei, M. He, Y. Zhang, Z. Wang, and D. Feng, "Improving spatial-spectral endmember extraction in the presence of anomalous ground objects," *IEEE Trans. Geosci. Remote Sens.*, vol. 49, pp. 4210–4222, 2011.

[54] J. M. P. Nascimento and J. M. B. Dias, "Does independent component analysis play a role in unmixing hyperspectral data?," *IEEE Trans. Geosci. Remote Sens.*, vol. 43, pp. 175–187, 2005.

[55] D. Seung and L. Lee, "Algorithms for non-negative matrix factorization," *Advances in Neural Information Processing Systems*, vol. 13, pp. 556–562, 2001.

[56] M. D. Iordache, J. M. Bioucas-Dias, and A. Plaza, "Sparse unmixing of hyperspectral data," *IEEE Trans. Geosci. Remote Sens.*, vol. 49, pp. 2014–2039, 2011.

[57] D. S. Huang and J. X. Mi, "A new constrained independent component analysis method," *IEEE Trans. Neural Netw.*, vol. 18, pp. 1532–1535, 2007.

[58] Z. L. Sun and L. Shang, "An improved constrained ICA with reference based unmixing matrix initialization," *Neurocomputing*, vol. 73, pp. 1013–1017, 2010.

[59] L. Miao and H. Qi, "Endmember extraction from highly mixed data using minimum volume constrained nonnegative matrix factorization," *IEEE Trans. Geosci. Remote Sens.*, vol. 45, pp. 765–777, 2007.

[60] S. Jia and Y. Qian, "Constrained nonnegative matrix factorization for hyperspectral unmixing," *IEEE Trans. Geosci. Remote Sens.*, vol. 47, pp. 161–173, 2009.

[61] K. C. M. Corresponding, L. Verbeke, E. Ducheyne, and R. De Wulf, "Using genetic algorithms in sub-pixel mapping," *Int. J. Remote Sens.*, vol. 24, pp. 4241–4247, 2003.

[62] G. Foody, "Sharpening fuzzy classification output to refine the representation of sub-pixel land cover distribution," *Int. J. Remote Sens.*, vol. 19, pp. 2593–2599, 1998.

[63] A. Tatem, H. Lewis, P. Atkinson, and M. S. Nixon, "Super-resolution land cover pattern prediction using a hopfield neural network," *Remote Sens. Environ.*, vol. 79, pp. 1–14, 2002.

[64] L. Zhang, K. Wu, Y. Zhong, and P. Li, "A new sub-pixel mapping algorithm based on a BP neural network with an observation model," *Neurocomputing*, vol. 71, pp. 2046–2054, 2008.

[65] Y. Zhong and L. Zhang, "Remote sensing image subpixel mapping based on adaptive differential evolution," *IEEE Trans. Syst., Man, Cybern., B: Cybernetics*, 2012.

[66] Y. Zhong, L. Zhang, L. Pingxiang, and H. Shen, "A sub-pixel mapping algorithm based on artificial immune systems for remote sensing imagery," in *Proc. 2009 IEEE Int. Geoscience and Remote Sensing Symp., IGARSS 2009*, pp. III-1007–III-1010.

[67] Y. F. Zhang, S. De Backer, and P. Scheunders, "Noise-resistant wavelet-based Bayesian fusion of multispectral and hyperspectral images," *IEEE Trans. Geosci. Remote Sens.*, vol. 47, pp. 3834–3843, Nov. 2009.

[68] Y. F. Gu, Y. Zhang, and J. P. Zhang, "Integration of spatial-spectral information for resolution enhancement in hyperspectral images," *IEEE Trans. Geosci. Remote Sens.*, vol. 46, pp. 1347–1358, May 2008.

[69] Z. Shi, Z. An, and Z. Jiang, "Hyperspectral image fusion by the similarity measure-based variational method," *Optical Eng.*, vol. 50, p. 077006, 2011.

[70] H. F. Shen, L. P. Zhang, B. Huang, and P. X. Li, "A MAP approach for joint motion estimation, segmentation, and super resolution," *IEEE Trans. Image Process.*, vol. 16, pp. 479–490, Feb. 2007.

[71] X. Jiang, L. Tang, C. Wang, and C. Wang, "Spectral characteristics and feature selection of hyperspectral remote sensing data," *Int. J. Remote Sens.*, vol. 25, pp. 51–59, 2004.

[72] S. Jia, Z. Ji, Y. Qian, and L. Shen, "Unsupervised band selection for hyperspectral imagery classification without manual band removal," *IEEE J. Sel. Topics Appl. Earth Observ. Remote Sens*, vol. 5, pp. 531–543, 2012.

[73] Y. Q. Zhao, L. Zhang, and S. G. Kong, "Band-subset-based clustering and fusion for hyperspectral imagery classification," *IEEE Trans. Geosci. Remote Sens.*, vol. 49, pp. 747–756, 2011.

[74] R. Huang and M. He, "Band selection based on feature weighting for classification of hyperspectral data," *IEEE Geosci. Remote Sens. Lett.*, vol. 2, pp. 156–159, 2005.

[75] Y. Zhong and L. Zhang, "An adaptive artificial immune network for supervised classification of multi-/hyperspectral remote sensing imagery," *IEEE Trans. Geosci. Remote Sens.*, vol. 50, pp. 894–909, 2012.

[76] Y. Zhong and L. Zhang, "Sub-pixel mapping algorithm based on adaptive differential evolution for remote sensing imagery," in *Proc. 2011 IEEE Int. Geoscience and Remote Sensing Symp., IGARSS 2011*, pp. 1724–1727.

[77] A. Plaza, J. A. Benediktsson, J. W. Boardman, J. Brazile, L. Bruzzone, G. Camps-Valls, J. Chanussot, M. Fauvel, P. Gamba, and A. Gualtieri, "Recent advances in techniques for hyperspectral image processing," *Remote Sens. Environ.*, vol. 113, pp. S110–S122, 2009.

[78] R. Zhang and J. Ma, "Feature selection for hyperspectral data based on recursive support vector machines," *Int. J. Remote Sens.*, vol. 30, pp. 3669–3677, 2009.

[79] X. Huang and L. Zhang, "Comparison of vector stacking, multi-SVMs fuzzy output, and multi-SVMs voting methods for multiscale VHR urban mapping," *IEEE Geosci. Remote Sens. Lett.*, vol. 7, pp. 261–265, 2010.

[80] Y. Chen and X. Li, "Kernel-based hierarchical cluster analysis," *J. Jilin University (Earth Science Edition)*, vol. 40, pp. 1211–1216, 2010.

[81] X. Huang and L. Zhang, "A comparative study of spatial approaches for urban mapping using hyperspectral ROSIS images over Pavia city, northern Italy," *Int. J. Remote Sens.*, vol. 30, pp. 3205–3221, 2009.

[82] X. Huang and L. Zhang, "An adaptive mean-shift analysis approach for object extraction and classification from urban hyperspectral imagery," *IEEE Trans. Geosci. Remote Sens.*, vol. 46, pp. 4173–4185, 2008.

[83] L. Zhang and X. Huang, "Object-oriented subspace analysis for airborne hyperspectral remote sensing imagery," *Neurocomputing*, vol. 73, pp. 927–936, 2010.

[84] Q. Yu, P. Gong, N. Clinton, G. Biging, M. Kelly, and D. Schirokauer, "Object-based detailed vegetation classification with airborne high spatial resolution remote sensing imagery," *Photogramm. Eng. Remote Sens.*, vol. 72, p. 799, 2006.

[85] C. Zhang and Z. Xie, "Combining object-based texture measures with a neural network for vegetation mapping in the everglades from hyperspectral imagery," *Remote Sens. Environ.*, vol. 124, pp. 310–320, 2012.

[86] Q. Tong, L. Zheng, and Y. Xue, "Development and application of hyperspectral remote sensing in China," in *Asia-Pacific Symp. Remote Sensing of the Atmosphere, Environment, and Space*, 1998, pp. 2–9.

[87] T. Qingxi, Z. Lanfen, J. Hao, W. Jinnian, T. Qingjiu, H. Hongfei, and Y. Jinshan, "The study for gold mineralization by thermal infrared multispectral scanner (TIMS)," *J. Infrared Millim. Waves*, vol. 11, pp. 249–256, 1992.

[88] S. Yan, B. Zhang, Y. Zhao, L. Zheng, Q. Tong, and K. Yang, "Summarizing the technical flow and main approaches for discrimination and mapping of rocks and minerals using hyperspectral remote sensing," *Remote Sens. Technol. Applicat.*, vol. 19, pp. 52–63, 2004.

[89] Q. Zhou, F. Gan, R. Wang, and J. Chen, "Mineral auto-identification based on hyperspectral imaging data and its application," *Remote Sensing for Land and Resources*, vol. 4, pp. 28–31, 2005.

[90] F. Gan and R. Wang, "The application of the hyperspectral imaging technique to geological investigation," *Remote Sensing for Land and Resources*, vol. 4, pp. 14–14, 2007.

[91] P. Hu, Q. Tian, and B. Yan, "The application of hyperspectral remote sensing to the identification of hydrocarbon alteration minerals in QAIDAM basin," *Remote Sensing for Land and Resources*, vol. 2, pp. 54–61, 2009.

[92] W. Sun, J. Chen, R. Wang, B. Yan, and H. Yu, "The application and research of hyperion for hyperspectral mineral mapping on east of Tianshan mountain," *Xinjiang Geology*, vol. 28, pp. 214–217, 2010.

[93] R. Wang, F. Gan, B. Yan, S. Yang, and Q. Wang, "Hyperspectral mineral mapping and its application," *Remote Sensing for Land and Resources*, vol. 1, pp. 1–13, 2010.

[94] S. Yan, X. Wu, C. Zhou, Z. Liu, Y. Zhuang, C. Cao, X. Wei, C. Yu, and C. Xiao, "Remote sensing and spectral geology and their applications to mineral exploration," *Advances in Earth Science*, vol. 26, pp. 13–29, 2011.

[95] X. Bi, F. Miao, B. Wu, J. Li, and D. Wang, "Hyperion hyperspectral remote sensing application in altered mineral mapping in East Kunlun of the Qinghai-Tibet Plateau," in *2010 Int. Conf. Challenges in Environmental Science and Computer Engineering (CESCE)*, 2010, pp. 519–523.

[96] F. Ye, D. Liu, and Y. Zhao, "Airborne hyperspectral survey system CASI/SASI and its preliminary application in uranium exploration," *World Nuclear Geoscience*, vol. 28, pp. 231–236, 2012.

[97] D.-Q. Xu, G.-Q. Ni, L.-L. Jiang, Y.-T. Shen, T. Li, S.-L. Ge, and X.-B. Shu, "Exploring for natural gas using reflectance spectra of surface soils," *Advances in Space Research*, vol. 41, pp. 1800–1817, 2008.

[98] Y. Z. Wu, X. Zhang, B. K. Yan, F. P. Gan, Z. S. Tang, A. A. Xu, Y. C. Zheng, and Y. L. Zou, "Global absorption center map of the mafic minerals on the moon as viewed by CE-1 IIM data," *Science China Physics, Mechanics & Astronomy*, vol. 53, pp. 2160–2171, 2010.

[99] Y. Wu, B. Xue, B. Zhao, P. Lucey, J. Chen, X. Xu, C. Li, and Z. Ouyang, "Global estimates of lunar iron and titanium contents from the Chang'E-1 IIM data," *J. Geophys. Res.*, vol. 117, p. E02001, 2012.

[100] J. Wang, L. Zhang, Q. Tong, and X. Sun, *The Spectral Crust Project—Research on New Mineral Exploration Technology*. Shanghai, China: WHISPER, 2012.

[101] G. Carr, A. Andrew, G. Denton, A. Giblin, M. Korsch, and D. Whitford, "The "Glass Earth"—Geochemical frontiers in exploration through cover," *AIG Bulletin*, vol. 28, pp. 33–40, 1999.

[102] S. U. Junying, "A spectrum fractal feature classification algorithm for agriculture crops with hyper spectrum image," *MIPPR 2011: Multispectral Image Acquisition, Processing, and Analysis*, vol. 8002, 2011.

[103] J. Wang, Y. H. Li, Y. Q. Chen, T. He, and C. Y. Lv, "Hyperspectral degraded soil line index and soil degradation mapping in agriculture-pasture mixed area in Northern China," in *Proc. Int. Workshop on Earth Observation and Remote Sensing Applications*, 2008, pp. 217–226.

[104] J. Wu and D. L. Peng, "Advances in researches on hyperspectral remote sensing forestry information-extracting technology," *Spectroscopy and Spectral Analysis*, vol. 31, pp. 2305–2312, Sep. 2011.

[105] Y. Keming, C. Yunhao, and G. Dazhi, "Spectral information detection and extraction of wheat stripe rust based on hyperspectral image," *Acta Photonica Sinica*, vol. 31, pp. 145–150, 2008.

[106] G. L. Tian and X. H. Yang, "Remote sensing model for wheat drought monitoring," *Remote Sens. Environ. (China)*, vol. 7, pp. 83–89, 1992.

[107] L. Y. Liu, "Hyperspectral remote sensing application in precision agriculture," Ph.D. dissertation, Institute of Remote Sensing Applications, Chinese Academy of Sciences, Beijing, China, 2002.

[108] L. Y. Liu, B. Zhang, L. F. Zheng, Q. X. Tong, Y. N. Liu, Y. Q. Xue, M. H. Yang, and C. J. Zhao, "Target classification and soil water content regression using surface temperature (LST) and vegetation index (VI)," *J. Infrared Millim. Waves*, vol. 21, pp. 269–273, 2002.

[109] Y. Y. Wang, Y. H. Chen, J. Chen, and W. J. Huang, "Two new red edge indices as indicatiors for stripe rust disease severity of winter wheat," *J. Remote Sens.*, vol. 11, pp. 875–881, 2007.

[110] L. Y. Liu, J. H. Wang, W. J. Huang, C. J. Zhao, B. Zhang, and Q. X. Tong, "Improving winter wheat yield prediction by novel spectral index," *Trans. CSAE*, vol. 20, pp. 172–175, 2004.

[111] P. Gong and R. L. Pu, "Conifer species recognition: Effects of data transformation," *Int. J. Remote Sens.*, vol. 22, pp. 3471–3481, Nov. 20, 2001.

[112] Y. Q. Zhang, J. M. Chen, J. R. Miller, and T. L. Noland, "Leaf chlorophyll content retrieval from airborne hyperspectral remote sensing imagery," *Remote Sens. Environ.*, vol. 112, pp. 3234–3247, Jul. 15, 2008.

[113] W. H. Zhao, B. H. Shan, and R. X. Zhong, "The normalized difference thermal index (NDTI) for the MODIS fire detection," *Remote Sens. Technol. Applicat.*, vol. 22, pp. 403–409, 2007.

[114] F. Gan, S. Liu, and Q. Zhou, "Identification of mining pollution using Hyperion data at Dexing copper mine in Jiangxi Province, China," *Earth Science—J. China University of Geosciences*, vol. 29, pp. 119–126, 2004.

[115] B. Zhang, D. Wu, L. Zhang, Q. J. Jiao, and Q. T. Li, "Application of hyperspectral remote sensing for environment monitoring in mining areas," *Environmental Earth Sciences*, vol. 65, pp. 649–658, Feb. 2012.

[116] F. L. Yan, S. X. Wang, Y. Zhou, and Q. Xiao, "Monitoring the water quality of Taihu lake by using Hyperion hyperspectral data," *J. Infrared Millim. Waves*, vol. 25, pp. 460–464, 2006.

[117] G. H. Zhou, Q. H. Liu, R. H. Ma, and G. L. Tian, "Inversion of chlorophyll—A concentration in turbid water of Lake Taihu based on optimized multi-spectral combination," *J. Lake Sci.*, vol. 20, pp. 153–159, 2008.

[118] D. Y. Sun, Y. M. Li, and Q. Wang, "A unified model for remotely estimating chlorophyll-a in Lake Taihu, China, based on SVM and in situ hyperspectral data," *IEEE Trans. Geosci. Remote Sens.*, vol. 47, pp. 2957–2965, Aug. 2009.

[119] Q. Shen, B. Zhang, and J. S. Li, "Study on level-1 requirements of hyperapectral remote sensing sensor for inland waters," presented at the WHISPERS 2012, Shanghai, China, 2012.

[120] X. Hu, B. Zhang, X. Zhang, Q. Tong, L. Zheng, Q. Wang, and J. Yu, "A new architecture for remote-sensing environmental monitoring system REMS: Design and implementation," in *Proc. IEEE Int. Geoscience and Remote Sensing Symp. (IGARSS)*, 2004, pp. 2115–2118.

[121] J. S. Li, "Study on retrieval of inland water quality parameters from hyperspectral remote sensing data by analytical approach—Taking Taihu Lake as an example," Ph.D. dissertation, Institute of Remote Sensing Applications, Chinese Academy of Sciences, Beijing, China, 2007.

[122] S. Li, L. Chen, F. Zheng, D. Han, and Z. Wang, "Design and application of Haze Optic Thickness retrieval model for Beijing Olympic Games," in *Proc. 2009 IEEE Int. Geoscience and Remote Sensing Symp., IGARSS 2009*, pp. II-507–II-510.

[123] D. Ji, Y. Wang, L. Wang, L. Chen, B. Hu, G. Tang, J. Xin, T. Song, T. Wen, Y. Sun, Y. Pan, and Z. Liu, "Analysis of heavy pollution episodes in selected cities of Northern China," *Atmospheric Environment*, vol. 50, pp. 338–348, 2012.

[124] J. Jiang, Y. Zha, J. Gao, and J. Jiang, "Monitoring of SO_2 column concentration change over China from Aura OMI data," *Int. J. Remote Sens.*, vol. 33, pp. 1934–1942, 2012.

[125] K. Wang, H. Jiang, X. Zhang, and G. Zhou, "Analysis of spatial and temporal variations of carbon dioxide over China using SCIAMACHY satellite observations during 2003–2005," *Int. J. Remote Sens.*, vol. 32, pp. 815–832, 2011.
[126] Z. Wang, L. Chen, J. Tao, Y. Zhang, and L. Su, "Satellite-based estimation of regional particulate matter (PM) in Beijing using vertical-and-RH correcting method," *Remote Sens. Environ.*, vol. 114, pp. 50–63, 2010.
[127] W. Xu, M. Wooster, and C. Grimmond, "Modelling of urban sensible heat flux at multiple spatial scales: A demonstration using airborne hyperspectral imagery of Shanghai and a temperature-emissivity separation approach," *Remote Sens. Environ.*, vol. 112, pp. 3493–3510, 2008.
[128] H. Yang, L. Zhang, X. Zhang, C. Fang, and Q. Tong, "Algorithm of emissivity spectrum and temperature separation based on TASI data," *Yaogan Xuebao—J. Remote Sens.*, vol. 15, pp. 1242–1254, 2011.
[129] H. Yang, "Study on temperature and emissivity separation from airborne hyperspectral thermal infraed data and their scale effect," Ph.D. dissertation, Graduate University of Chinese Academy of Sciences, Beijing, China, 2011.
[130] B. Zhang, "Hyperspectral data mining supported by temporal and spatial information," Ph.D. dissertation, Institute of Remote Sensing Applications, Chinese Academy of Sciences, Beijing, China, 2002.
[131] Y. D. Fan, Q. Wen, and S. R. Chen, "Engineering survey of the environment and disaster monitoring and forecasting small satellite constellation," *Int. J. Digital Earth*, vol. 5, pp. 217–227, 2012.
[132] Y. J. Cui, J. G. Du, Z. Chen, J. Li, C. Xie, X. Zhou, and L. Liu, "Remote sensing signals of atmospheric physics and chemistry related to 2010 Yushu Ms 7.1 earthquake," *Advances in Earth Science*, vol. 26, pp. 787–794, 2011.
[133] W. H. Pang, J. J. Chen, H. Chen, C. G. Zhang, and L. C. Li, "Dynamic monitoring of drought in Fujian Province from MODIS remote sensing data," *Chinese J. Eco-Agriculture*, vol. 16, pp. 1015–1019, 2008.
[134] Y. L. Weng and P. Gong, "Remote sensing research progress of soil salinization," *Geograph. Sci.*, vol. 26, pp. 369–375, 2006.
[135] Y. D. Fan, L. Wang, J. Nie, W. Wang, and B. J. Zhang, "Remote sensing monitoring and assessment technology for cryogenic freezing rain and snow disasters in China: Research and application," *J. Natural Disasters*, vol. 17, pp. 21–25, 2009.
[136] H. X. He, S. Y. Yang, W. T. Chen, H. Huang, Y. Cui, and X. P. Xie, "Application of HJ-1A hyperspectral data to the disaster reduction," *Spacecraft Eng.*, vol. 20, pp. 118–125, 2012.
[137] R. Waring, J. Landsberg, and M. Williams, "Net primary production of forests: A constant fraction of gross primary production?," *Tree Physiol.*, vol. 18, pp. 129–134, 1998.
[138] C. Wu, Z. Niu, Q. Tang, W. Huang, B. Rivard, and J. Feng, "Remote estimation of gross primary production in wheat using chlorophyll-related vegetation indices," *Agricult. Forest Meteorol.*, vol. 149, pp. 1015–1021, 2009.
[139] C. Wu, "Use of a vegetation index model to estimate gross primary production in open grassland," *J. Appl. Remote Sens.*, vol. 6, p. 063532-1, 2012.
[140] C. Y. Wu, J. M. Chen, and N. Huang, "Predicting gross primary production from the enhanced vegetation index and photosynthetically active radiation: Evaluation and calibration," *Remote Sens. Environ.*, vol. 115, pp. 3424–3435, Dec. 15, 2011.
[141] C. Y. Wu, J. W. Munger, Z. Niu, and D. Kuang, "Comparison of multiple models for estimating gross primary production using MODIS and eddy covariance data in Harvard forest," *Remote Sens. Environ.*, vol. 114, pp. 2925–2939, Dec. 15, 2010.
[142] C. Y. Wu, Z. Niu, and S. A. Gao, "Gross primary production estimation from MODIS data with vegetation index and photosynthetically active radiation in maize," *J. Geophys. Res.-Atmospheres*, vol. 115, Jun. 30, 2010.
[143] C. Y. Wu, X. Z. Han, J. S. Ni, Z. Niu, and W. J. Huang, "Estimation of gross primary production in wheat from in situ measurements," *Int. J. Appl. Earth Observ. Geoinf.*, vol. 12, pp. 183–189, Jun. 2010.
[144] M. Shen, Y. Tang, J. Klein, P. Zhang, S. Gu, A. Shimono, and J. Chen, "Estimation of aboveground biomass using in situ hyperspectral measurements in five major grassland ecosystems on the Tibetan plateau," *J. Plant Ecol.*, vol. 1, pp. 247–257, 2008.
[145] L. F. Zhang, "The universal pattern decomposition method and the vegetation index based on the UPDM," Ph.D. dissertation, Wuhan University, Wuhan, China, 2005.
[146] L. Zhang, S. Furumi, K. Muramatsu, N. Fujiwara, M. Daigo, and L. Zhang, "A new vegetation index based on the universal pattern decomposition method," *Int. J. Remote Sens.*, vol. 28, pp. 107–124, 2007.
[147] L. Zhang, N. Fujiwara, S. Furumi, K. Muramatsu, M. Daigo, and L. Zhang, "Assessment of the universal pattern decomposition method using MODIS and ETM+ data," *Int. J. Remote Sens.*, vol. 28, pp. 125–142, 2007.
[148] L. Zhang, B. Liu, B. Zhang, and Q. Tong, "An evaluation of the effect of the spectral response function of satellite sensors on the precision of the universal pattern decomposition method," *Int. J. Remote Sens.*, vol. 31, pp. 2083–2090, 2010.
[149] J. W. Zhao, K. L. Wang, Q. Ouyang, and Q. S. Chen, "Measurement of chlorophyll content and distribution in tea plant's leaf using hyperspectral imaging technique," *Spectroscopy and Spectral Analysis*, vol. 31, pp. 512–515, Feb. 2011.
[150] C. Zhao, Z. Wang, J. Wang, W. Huang, and T. Guo, "Early detection of canopy nitrogen deficiency in winter wheat (Triticum aestivum L.) based on hyperspectral measurement of canopy chlorophyll status," *New Zealand J. Crop Horticult. Sci.*, vol. 39, pp. 251–262, 2011.
[151] X. G. Xu, X. H. Gu, X. Y. Song, C. J. Li, and W. J. Huang, "Assessing rice chlorophyll content with vegetation indices from hyperspectral data," *Computer and Computing Technologies in Agriculture IV, Pt. 1*, vol. 344, pp. 296–303, 2011.
[152] S. Chen, S. Zhang, X. Sun, and Z. Li, "Quantitative estimation of rice chlorophyll concentration based on hyperspectral remote sensing technology," in *Proc. 2011 Int. Conf. Agricultural and Biosystems Engineering—Advances in Biomedical Engineering*, 2011, vol. 1-2, pp. 354–356.
[153] J. Y. Shi, X. B. Zou, J. W. Zhao, and X. P. Yin, "Measurement of chlorophyll distribution in cucumber leaves based on hyperspectral imaging technique," *Chinese J. Analyt. Chem.*, vol. 39, pp. 243–247, Feb. 2011.
[154] Z. Niu, H. Zhang, and P. Gong, "More protection for China's wetlands," *Nature*, vol. 471, pp. 305–305, 2011.
[155] B. Zhang, X. Wang, J. Liu, L. Zheng, and Q. Tong, "Hyperspectral image processing and analysis system (HIPAS) and its applications," *Photogramm. Eng. Remote Sens.*, vol. 66, pp. 605–609, 2000.
[156] H. Xingtang, "The research on the key technology of hyperspectral remote sensing enviroment monitoring system and its applications to water resources," Ph.D. dissertation, Graduate University of Chinese Academy of Sciences, Beijing, China, 2005.
[157] S. Yanmin, Z. Qijiang, W. Peijuan, W. Jindi, L. Suhong, and B. Xianghua, "Research on design of data warehouse system for object spectrum," *Comput. Eng. Applicat.*, vol. 39, pp. 199–201, 2003.
[158] H. Qin and L. Zhang, "Design of hyperspectral multidimensional database for rock and mineral," in *Proc. 2011 Int. Conf. Remote Sensing, Environment and Transportation Engineering (RSETE)*, 2011, pp. 1092–1095.

Qingxi Tong received the B.S. degree in agrometeorology from Odessa's Institute of Hydrometeorology, Former USSR.

He has been engaged in the study on the development and application of remote sensing since the beginning of 1970. He was elected as a Member of Chinese Academy of Sciences in 1997 and Academician of International Eurasian Academy of Sciences in the same year. Mr. Tong is one of the principal scientists in remote sensing in China. He has made outstanding contribution in development of remote sensing technology and applications, especially in development of airborne remote sensing system, and in study of remote sensing spectral properties of earth resources and environments. He serves as the chairman of the Expert Committee of National Remote Sensing Center of China (NRSCC), the Ministry of Science and Technology of China, associate editor of the *Journal of Remote Sensing*, and editorial committeeman of the Chinese *Journal of Space Science*. He is also active in international cooperation. Currently he is a chief scientist in cooperation project for development of small satellite of NRSCC and Surrey Space Center of UK (SSTL). As a result, a high performance small satellite named "Beijing-1" has been launched and successfully operated.

Prof. Tong was awarded the Prizes for Progress of Science and Technology of National and CAS many times due to his achievements. He was also awarded the prize of "Achievement for International Remote Sensing Science and Technology" by the SPIE in 2002.

Yongqi Xue was born in Zhangjiagang, Jiangsu Province in January 1937. He graduated from Faculty of Physics of the East China Normal University in 1959.

He is currently a Research Professor of Shanghai Institute of Technical physics, Chinese Academy of Sciences, Beijing, and is an infrared and remote sensing technique specialist. He was elected as academician of the Chinese Academy of Sciences in 1999. He has been engaged in infrared acquisition and multispectral remote sensing technique for more than 30 years. He successfully developed infrared scanners, multispectral scanners, imaging spectrometer, hyper imaging system one after another, and provided several types of advanced remote sensing means for the foundation of China's operational airborne remote sensing system and promoted the application of remote sensing technique in China. Remarkable results have been obtained in the applications of airborne remote sensing instrument in tree fire monitoring, geology remote sensing, marine pollution monitoring, precision agriculture, hydrology, archaeology, etc. Being the first in China to develop the three-dimension imaging remote sensing technique, he combined the scanning spectral imaging with laser scanning ranging and realized fast forming digital elevation model and geo-reference images without ground control points which are particularly suitable for beach, desert, grasslands, islands and so on, where there are poor transport facilities. This is a real-time and high effective new remote sensing system.

Lifu Zhang (S'04–M'05) received the B.E. degree in photogrammetry and remote sensing from the Department of Airborne Photogrammetry and Remote Sensing, Wuhan Technical University of Surveying and Mapping (WTUSM), Wuhan, China, in 1992, the M.E. degree in photogrammetry and remote sensing from the State Key Laboratory of Information Engineering in Surveying, Mapping and Remote Sensing, WTUSM, Wuhan, China, in 2000, and the Ph.D. degree in photogrammetry and remote sensing from the State Key Laboratory of Information Engineering in Surveying, Mapping and Remote Sensing, Wuhan University, Wuhan, China, in 2005.

He was a Visiting Researcher with the Department of Information and Computer Sciences, Nara Women's University, Nara, Japan, from 2003 to 2004, a Postdoctoral Researcher with the Institute of Remote Sensing and Geographic Information System, School of Earth and Space Sciences, Peking University, Beijing, China, from 2005 to 2007, and an Advanced Visiting Researcher with the Earth Science and Resource Engineering, Commonwealth Scientific and Industrial Research Organization (CSIRO), Sydney, Australia, in 2011. In 2007, he joined the Institute of Remote Sensing Applications (IRSA), Chinese Academy of Sciences (CAS), where he is currently a Professor and the Head of the Hyperspectral Remote Sensing Laboratory. His main research interests focus on hyperspectral remote sensing, imaging spectrometer system development and its applications etc.

Dr. Zhang is a member of SPIE and the Academy of Space Science of China and is also a committeeman of Chinese National Committee of the International Society for Digital Earth (CNISDE), a vice chairman of hyperspectral earth observation committee (HEOC) of CNISDE, and a Standing Committeeman of the Expert Committee of China Association of Remote Sensing Applications.